

Non-overlapping neural networks in *Hydra vulgaris*

Christophe Dupre

Submitted in partial fulfillment of the
Requirements for the degree of
Doctor of Philosophy
under the Executive Committee
of the Graduate School of Arts and Sciences

COLUMBIA UNIVERSITY

2018

© 2017

Christophe Dupre

All rights reserved

ABSTRACT

Non-overlapping neural networks in *Hydra vulgaris*

Christophe Dupre

To understand the emergent properties of neural circuits it would be ideal to record the activity of every neuron in a behaving animal and decode how it relates to behavior. We have achieved this with the cnidarian *Hydra vulgaris*, using calcium imaging of genetically engineered animals to measure the activity of essentially all of its neurons. While the nervous system of *Hydra* is traditionally described as a simple nerve net, we surprisingly find instead a series of functional networks that are anatomically non-overlapping and are associated with specific behaviors. Three major functional networks extend through the entire animal and are activated selectively during longitudinal contractions, elongations in response to light and radial contractions, while an additional network is located near the hypostome and is active during nodding. Additionally, we show that the behavior of *Hydra* is made of regularly occurring radial contractions, which expel the content of the gastric cavity about every 45 minutes. These results demonstrate the functional sophistication of apparently simple nerve nets, and the potential of *Hydra* and other basal metazoans as a model system for neural circuit studies.

CONTENTS

List of charts, graphs, illustrations	ii
Acknowledgements	iii
Introduction	1
Anatomy.....	1
Physiology – Electrical recordings.....	2
Hydra as an animal model in modern neurobiology	6
Results.....	9
Imaging the complete activity of the nervous system of Hydra	9
Functional networks of neurons in Hydra	18
RP1 and CB networks are ectodermal while RP2 is endodermal.....	23
RP1 is associated with elongations and RP2 with radial contractions.....	29
Subtentacle network is associated with nodding	33
Neuronal activity can propagate in 2 directions and at 2 different speeds in tentacles.....	36
Discussion	38
Hydra as a novel preparation for whole nervous system imaging	38
Nonoverlapping coactive networks of neurons in the nerve nets of Hydra.....	40
Two rhythmic potentials networks.....	41
Bidirectional propagation in the subtentacle network.....	43
Multiple conduction speeds	43
Broader relevance to neuroscience.....	44
Introduction	45
Experimental procedures.....	54
Hydra maintenance.....	54
Transgenics	54
Imaging.....	54
Pseudocoloring	56
Electrophysiology.....	56
Statistical methods.....	56
References	57
Appendix: Supplemental figures.....	61

LIST OF CHARTS, GRAPHS, ILLUSTRATIONS

Figure 1: Anatomy of Hydra.....2
Figure 2: Electrical activity in Hydra.....3
Figure 3: Synapses in Hydra seen with electron microscopy5
Figure 4: Imaging the entire nervous system activity of Hydra15
Figure 5: Simultaneous recording of electrical activity and calcium imaging.....17
Figure 6: The nervous system of Hydra includes three major networks.....22
Figure 7: Anatomical differences between the three major networks.....28
Figure 8: Behavioral association of two rhythmic potentials networks.....32
Figure 9: Subtentacle network (STN) causes nodding behavior and can conduct signal in both directions35
Figure 10: Signal propagates in both directions and at two different speeds in tentacles.....37
Figure 11: Thickness measurement46
Figure 12: Detection of radial contractions.....47
Figure 13: Detection of longitudinal contractions48
Figure 14: Continuous thickness measurement over 3 days50
Figure 15: Other cnidarians have transgenic capabilities53

ACKNOWLEDGEMENTS

I would like to thank Sydney Brenner for suggesting to work on *Hydra*, and Charles David, Rob Steele and Celina Juliano who provided an enormous amount of help in getting me started to make transgenic lines of *Hydra* and getting in touch with the *Hydra* community. Additionally, it was inspiring to be in touch with prof. Mac Passano, Gaby Kass-Simon and George Mackie because of their pioneering work in the field. I would like to thank all the present and past members of the Yuste lab with whom I ever interacted for their support and for being wonderful colleagues. The project I presented here also particularly benefitted from the help of Sanjana Salwi, Stephen Leong and Kaniz Fatema for help with neuron tracking. This work was supported by NIH Pioneer award DP1EY024503 (RY), DARPA award DARPA-HR0011-17-C-0026, U. S. Army Research Laboratory and the U. S. Army Research Office (Contract W911NF-12- 1-0594, MURI).

INTRODUCTION

Anatomy

The anatomy of *Hydra* is fairly simple when compared to most other multicellular animal models as it is radially symmetrical (Figure 1). The hypostome (unique opening of the gastric cavity) is surrounded with tentacles, and the body column forms a cylinder that attaches to the substrate via a peduncle. A cross-section of the body column reveals three layers of cells: endoderm, ectoderm and interstitial cells. The endoderm and ectoderm of the animal are made of epithelial cells that have muscular processes or myofilaments. The interstitial cells are made of multiple types of cells: gland cells, neurons and nematocytes[1]. A well-fed animal may measure up to 1.5 cm, whereas a starved animal can shrink down to less than a mm. Multiple other parameters such as the genetic strain and ambient temperature will affect the animal's size.

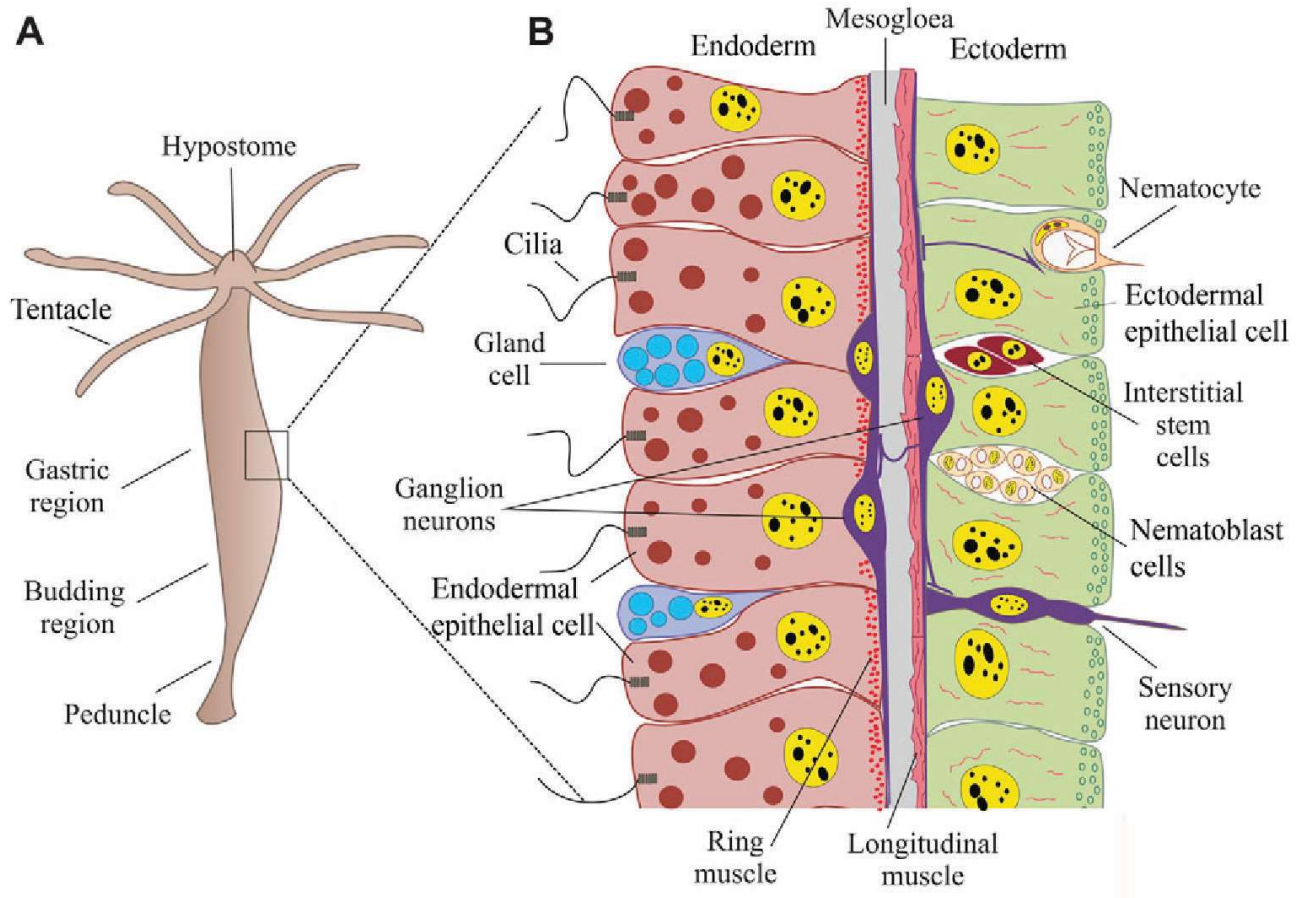


Figure 1: Anatomy of *Hydra*

A) Full animal, not sexually differentiated. A sexually differentiated animal will have one or multiple gonads, which will be testes and/or ovaries. B) Tissue section from the region boxed in A). The name of each cell type known to date is indicated, although there might be more cell types to be discovered. The connection between neurons in the endoderm and neurons in the ectoderm has not been identified yet. Reproduced from [1].

Physiology – Electrical recordings

Before functional imaging was available, the method of choice for measuring neuronal activity was electrophysiology. L.M. Passano and C. B. MacCullough undertook a series of experiments

in the 1960s that aimed at recording electrical activity in *Hydra* (Figure 2). They used suction electrodes that they would attach to the body of *Hydra* under different conditions. They observed that at rest, the animal generates two different types of spikes: short spikes and tall spikes. The tall spikes are organized as bursts and their occurrence matches the expression of a very stereotyped behavior: the contraction burst. The short spikes can occur in the absence of any behavior and were called rhythmic potentials (RPs). The interval between 2 RPs is pretty constant, but it can be modulated by a photic stimulus. Indeed, if an animal is dark-habituated it will elongate as soon as it is exposed to light. Moreover, during this elongation one can observe a transient increase in RP frequency [2].

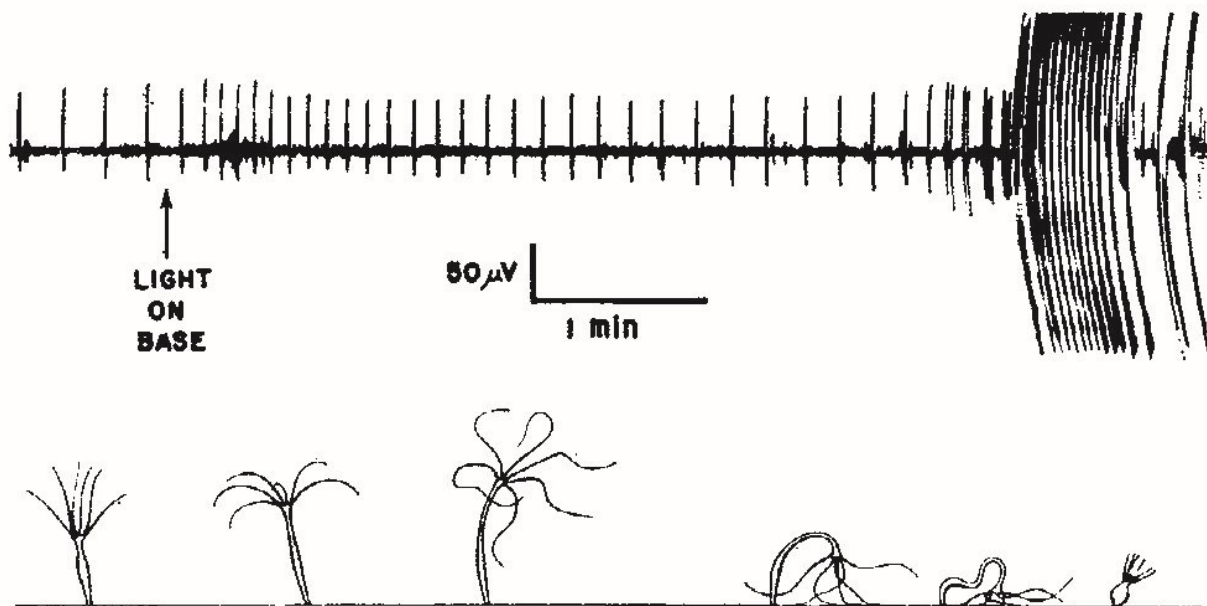


Figure 2: Electrical activity in *Hydra*

The trace on the top is the electrical signal recorded by Passano and McCullough when they placed a suction electrode against the body of the animal. One can see two types of spikes, tall and short, in this recording. Additionally, even though the short spikes occur at a regular interval their frequency can be modulated by a brief exposure to light, when the animal has been

previously habituated to darkness. This brief exposure to light triggers a behavior called elongation response. The bottom drawings represent different behaviors that *Hydra* can execute. The elongation response is represented by the first three drawings, whereas somersaulting and contraction bursts are represented by the 4th-5th and last drawing, respectively. Reprinted from [3].

Physiology – synapses

The type of synapse used by the neurons of *Hydra* in order to connect to each other has been studied mostly with electron microscopy. As a result, both chemical and electrical synapses were found (Figure 3), connecting neurons to each other but also connecting neurons with epithelial cells. These synapses were observed in multiple parts of the body of the animal, including the hypostome, peduncle and body column. The chemical synapses of *Hydra* seem to be using a high density of dense core vesicles when compared to mammalian chemical synapses, although small synaptic vesicles are also visible under electron microscopy. Another particularity of these synapses is that many of them seem to be bidirectional, i.e. containing vesicles in both the pre and postsynaptic compartments [4–8].

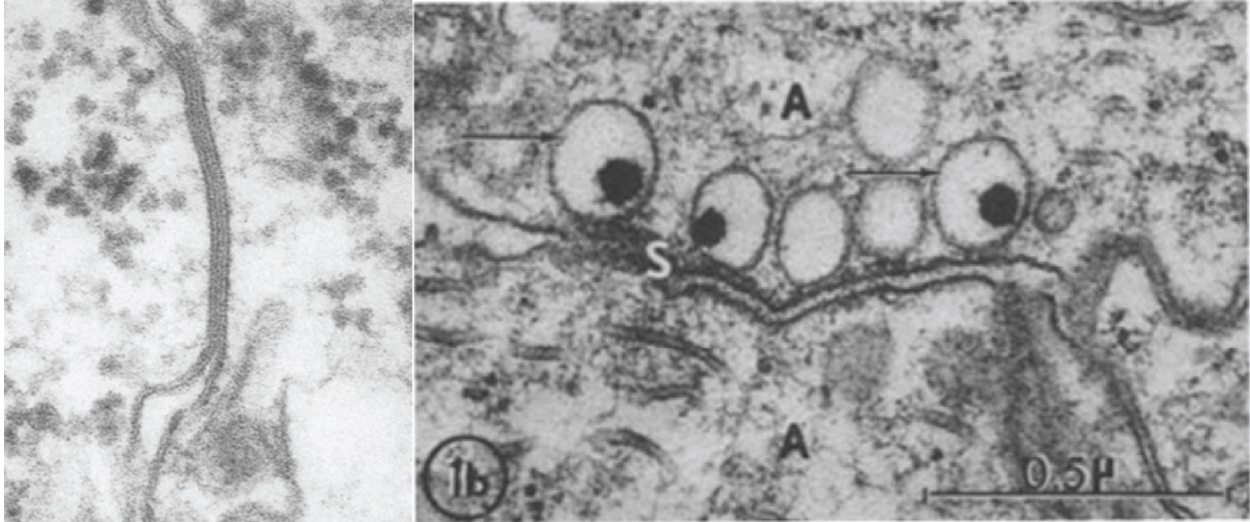


Figure 3: Synapses in *Hydra* seen with electron microscopy

Left: gap junction with high density of ribosomes nearby. Magnification x 118,000. Reproduced from [5]. Right: chemical synapse (S) with two neurites (A) and dense core vesicles (arrows). Reproduced from [4].

Discovery and early research

Since its discovery in 1702 by Antony Van Leeuwenhoek [9], *Hydra* has been used as an animal model to improve our understanding of biological processes. In 1744, Trembley published his *Mémoires* book, where he described for the first time (together with experiments) asexual reproduction by budding, the first controlled experiments in animals on regeneration, the first successful animal grafts, first study of phototaxis in animals without eyes, and the first vital staining of tissues [10].

Ethel Browne also contributed major advances in our understanding of developmental biology as she was a graduate student. Indeed, working under Thomas Hunt Morgan she used *Hydra* to demonstrate the organizer phenomenon for the first time [11]. She showed that when grafting the tentacle of a *Hydra* onto the body column of another *Hydra*, one can trigger the growth of a new

Hydra at the grafting site. This new *Hydra* will develop normally as if it had been the result of budding or asexual reproduction. These experiments were done prior to the experiments by Spemann and Mangold, but did not receive the same amount of attention [11].

Hydra as an animal model in modern neurobiology

Understanding the function of any nervous system is a daunting task given the number of neurons involved and the difficulty in measuring and analyzing their activity. Cnidarians, as a sister group of bilaterians, are extant representative of some of the earliest animals in evolution to have nervous systems and thus offer an apparent simplicity that could help illuminate the structural and functional design principles of neural circuits. Among cnidarians, *Hydra* is convenient to maintain and manipulate in a laboratory and, consequently, has been studied for more than 300 years [9]. The nervous system of *Hydra* is composed of a few hundred to a few thousand neurons, depending on the size of the animal [12]. Two main types of neurons have been reported: sensory cells, exposed to the external or gastric environment, and ganglion cells, which form a two-dimensional lattice known as nerve net [8,13]. *Hydra's* nerve net has actually two separate components: one in the endoderm and one in the ectoderm. The morphology of both sensory cells and ganglion cells can vary, in terms of the size of their cell body and the ramification of their neurites [14].

The function of nerve nets in *Hydra* is poorly understood. Extracellular recordings reported multiple types of electrical activity, some of which are associated with motion or occur in response to sensory stimulation. Specifically, longitudinal contraction of the ectoderm, which reduces the animal down to a tight ball, is associated with a type of extracellular electrical signals named longitudinal contraction bursts (CB) [2]. Tentacles sometimes also generate electrical pulses

(tentacle pulses), found during contractions [15,16]. But in addition, *Hydra* displays robust spontaneous electrical activity, i.e. activity in the apparent absence of any external stimulus and, sometimes, also in the absence of any clear behavior. One example of this are the rhythmic electrical potentials [2,17], which have been thought to propagate in the endoderm of the animal [18] and to increase in frequency during elongation of the body column [2]. Activation of the endoderm by rhythmic potentials is thought to cause radial contraction (reduction of the radius of the animal) and therefore elongation [19,20].

Hydra has a limited and well-characterized behavioral repertoire, including photic response and feeding. A dark-habituated *Hydra* that is exposed to light will respond by elongating its body towards it, bending its hypostome-tentacle junction to produce a motion reminiscent of nodding [3,21], and eventually moving towards the light source by somersaulting [10]. Feeding includes a combination of tentacle motion to spear and paralyze the prey with nematocysts in order to bring the prey towards the mouth, which opens to ingest it [22]. A few hours after ingestion, the content of the body column is expelled through the mouth by a quick radial (as opposed to longitudinal) contraction of the body column after the mouth has opened [23].

Elucidation of the links between neuronal activity, anatomy and behavior in *Hydra* has been difficult because of technical limitations. Single-cell recording approaches are difficult because *Hydra* neurons are small and scattered [24], although intracellular recordings reveal action potentials [25]. Extracellular studies have provided detailed descriptions of electrical signals but could not link them to a particular cell type. In fact, whether rhythmic potentials and longitudinal contraction bursts are conducted by neurons or by the muscle/epithelial cells is still under debate [18,26,27], and surgical isolations indicate that they can propagate along both axes of the epithelium [16]. Also, extracellular recordings, which could be more akin to electromyograms, can

be disrupted by the motion of the animal [17], and therefore cannot be carried out in certain types of behavior. Accordingly, one does not know how many networks exist in the nervous system of *Hydra* and to what behavior each of them participates.

The application of modern molecular methods to *Hydra* has the potential to greatly advance our understanding of these essential neurobiological questions. In particular, the recent sequencing of *Hydra* has revealed a surprisingly rich genome [28]. Indeed, in spite of its basal metazoan lineage, the *Hydra* genome is endowed with more than 20,000 genes including an extensive complement of neuronal molecular families such as sodium, potassium and calcium channels, and receptors for glutamate, GABA, Dopamine, 5HT, and many peptides. Many of these molecules are even present in animals that are evolutionary more basal than cnidarians, such as the poriferans (sponges) [29]. Also, stable transgenic lines have been achieved [30], enabling the use of a large range of modern molecular tools. Among these tools, genetically-encoded calcium indicators are particularly well suited for functional studies of the *Hydra* nerve net for many reasons. First, calcium imaging can track the action potential activity of neuronal populations [31]. Second, the small size of *Hydra* (500 μm to 1.5 cm in length) makes it possible to have an entire animal under the field of view of a traditional microscope. Third, *Hydra* is transparent and its scattered nerve-net organization (disadvantageous for electrophysiological recordings) is advantageous for imaging. Indeed, it is rare that two neurons optically overlap during imaging so it is therefore easier to obtain single-neuron resolution. Fourth, *Hydra* does not age [32], so the same animal can be used in an indefinite number of experiments. This can reduce the number of confounding factors and make statistical interpretation more accurate. Fifth, *Hydra* regenerates which makes it more robust against photodamage. Other cnidarians are available, such as *Hydractinia*, *Aglantha* and *Nematostella*. These animals offer various advantages, such as the broad range of genetic tools

that are available in *Nematostella* [33]. In spite of the fact that these species might not have the same optical advantages as *Hydra*, running similar experiments in them would offer exciting comparative perspectives between the nervous system of anthozoans (e.g. *Nematostella*) and hydrozoans (e.g. *Hydra*). To take advantage of these properties and explore the possibility of performing neural circuit studies of *Hydra*, we created a line expressing a calcium indicator (GCaMP6s) in neurons. Using it, we attempted to link neuronal activity with the anatomy of the nerve net and the behavior of the animal.

RESULTS

Imaging the complete activity of the nervous system of Hydra

In order to record the activity of the entire nervous system of *Hydra* simultaneously we first generated a line of transgenic animals expressing a genetic calcium indicator and then developed a method to image whole individuals. To generate the transgenic line, we modified a plasmid initially designed by R. Steele (UC Irvine; Addgene cat#34789) [34] and which expresses GFP under the control of an actin promoter. In the sequence of this plasmid, we substituted GCaMP6s for GFP (see Supplemental Material). We then injected the plasmid in fertilized *Hydra* eggs (Figure 4A) according to an established procedure [35] (see also Supplemental Experimental Procedures), with the goal of incorporating the plasmid into the interstitial cell lines, which give rise to the neuronal lineage.

Animals generated were mosaic, with transgenic stem cells randomly scattered throughout the body. By repeatedly selecting buds that formed on a region of the parent that has higher concentration of transgenic stem cells than the rest of the body of the parent, we progressively increased the percentage of transgenic neurons in our colony. Once the percentage of transgenic

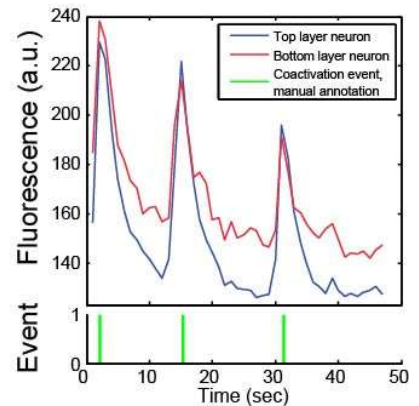
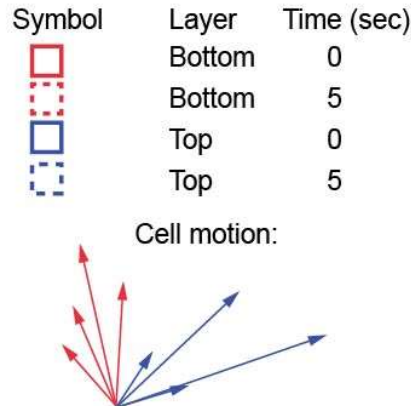
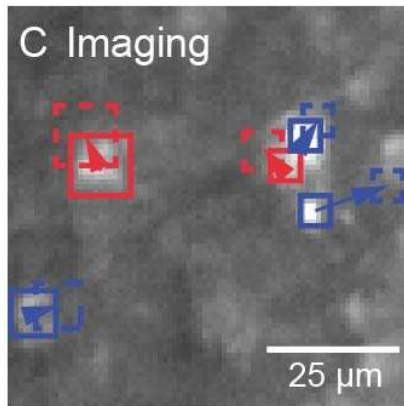
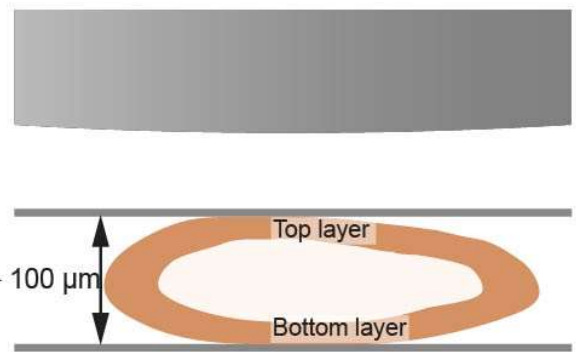
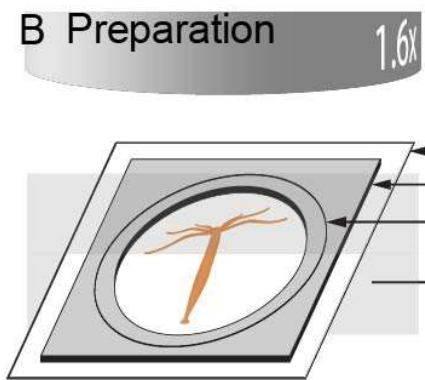
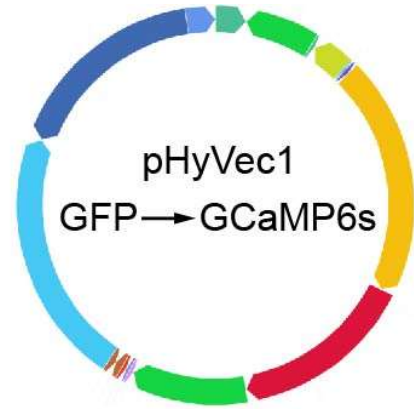
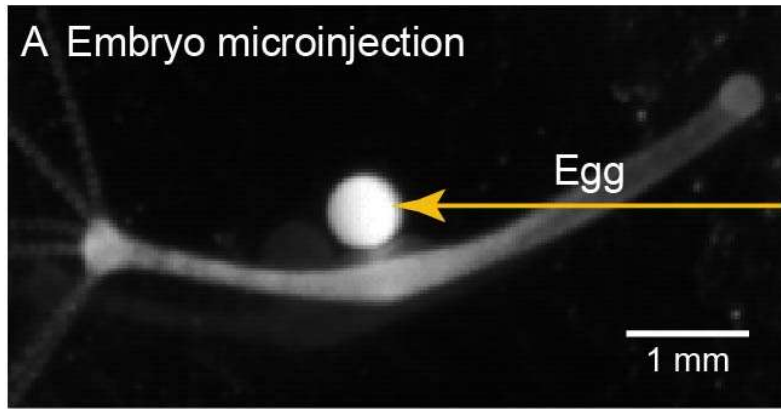
neurons seemed to have reached a steady-state, we measured it by immunostaining animals for GCaMP6s (using a GFP antibody) and acetylated alpha tubulin, a pan-neuronal marker [36]. In these animals, 96 ± 3 (SEM) % of cells positive for acetylated alpha tubulin also expressed GCaMP6s (see Figure S1). Since it is likely that a small percentage of neurons might not have been stained for GFP and/or for anti-acetylated alpha tubulin during the immunohistochemistry procedure, we concluded that the transgenic lines expressed GCaMP6s in essentially all of its neurons.

To image the activity of every neuron in the animal, we mounted specimens between two coverslips separated by a $100\mu\text{m}$ spacer, which is the average width of a small *Hydra* (Figure 4B) and imaged in wide-field mode at max 33Hz frame rate (Movie S1; cf experimental procedures). In such preparation, the animal can be considered as a hollow cylinder that is imaged from the side, between the top coverslip (top layer in Figure 4B), and the bottom coverslip (bottom layer in Figure 4B). Consequently, we expected to see two layers of neurons (the two sides of the cylinder) slide on top of each other as the animal is moving in this chamber. Indeed, we could identify the two body walls by measuring the trajectory of 8 neurons in a given region of interest, and plotting these trajectories on top of each other (Figure 4C, left and middle panels). Accordingly, the 8 trajectories essentially followed two different directions corresponding to the motion of the two layers of the animal. Moreover, we could detect calcium transients from neurons in both layers (Figure 4C, right panel). We ruled out the possibility that these fluorescence transients come from motion of the cells in and out of focus by comparing them to the signal we acquired from animals expressing GFP (rather than GCaMP6s) in neurons (Figure S2). For these reasons, we can conclude that our preparation allows us to image neuronal activity through the entire animal simultaneously.

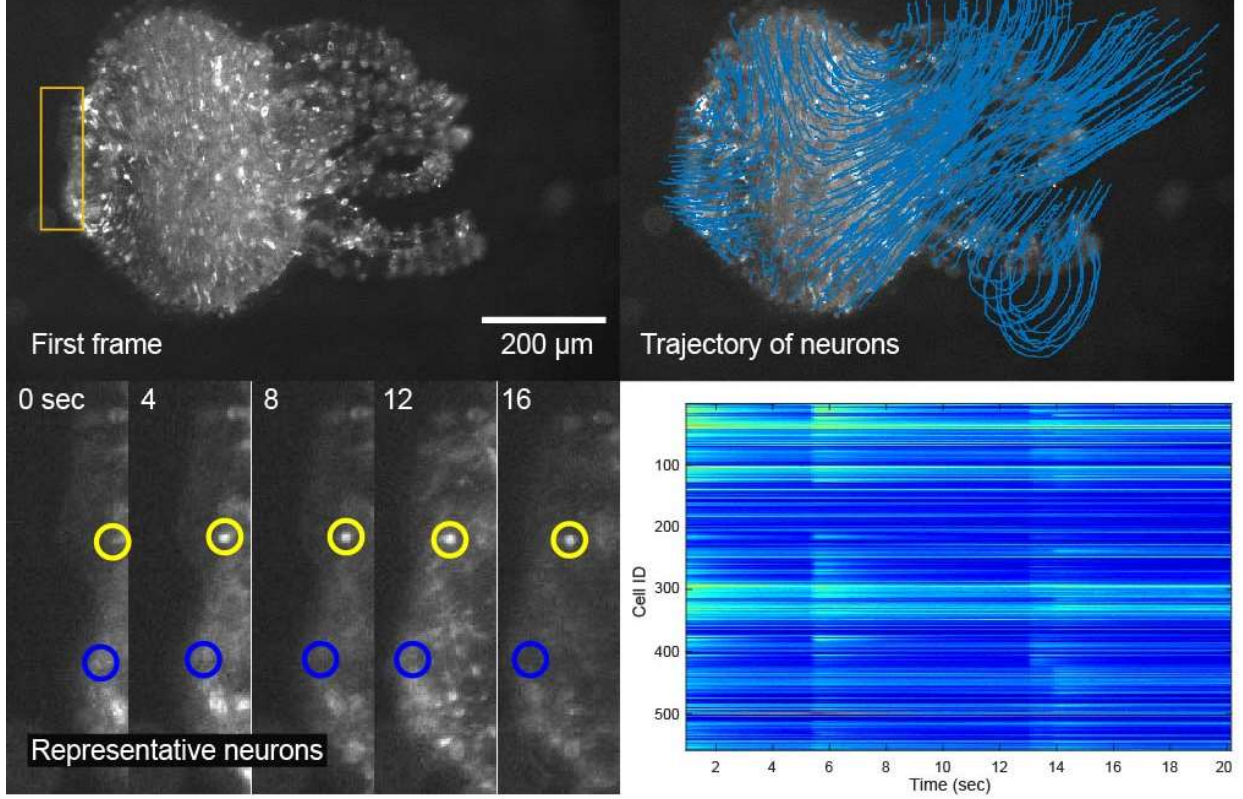
In order to extract neuronal activity in spite of the motion of the animal, we manually tracked the trajectory of each neuron and measured their fluorescence intensity at each frame (cf experimental procedures; Figure 4D and Movie S2). Additionally, we attempted to correlate calcium signal with electrical activity of the neurons by approaching extracellular electrodes (Figure 5A). We were not able to record the electrical activity of CB neurons, because whenever they fired the electrical signal generated by the contracting muscles overwhelmed any other signal (Figure 5B). However, we were able to record electrical signals from rhythmic potentials neurons, because they can occur when the animal does not move. The calcium transients we observed all had the same amplitude, and the electrical activity that corresponded to them always involved a single spike (Figure 5C-D). Therefore, each RP calcium transient corresponded to one action potential.

Using these traces for each neuron, we built rasterplots representing the activity of every neuron over hundreds of frames (Figure 4D). Note that each animal can have a different number of neurons, as *Hydra* can grow and shrink depending on its food intake [12]. In addition, we tested how fast and for how long we could image these animals in our preparation. The duration of recording was limited by photobleaching and phototoxicity, which we assessed by measuring fluorescence intensity and neuronal activity, respectively. The speed of recording in our preparation was limited by the minimum acquisition time of the camera (30ms). At this maximum speed, it was possible to continuously record neuronal activity for more than one hour without any apparent toxicity and little bleaching (Figure 4E). Because our staining indicates that every neuron was transgenic and our recording technique could image both layers of the animal, we believe to be close to imaging the activity of every neuron of *Hydra* simultaneously. Using these recordings,

we classified the neurons of *Hydra* according to their morphologies, activity patterns, or any behavior observed.



D Manual tracking of neurons



E Long-term recording

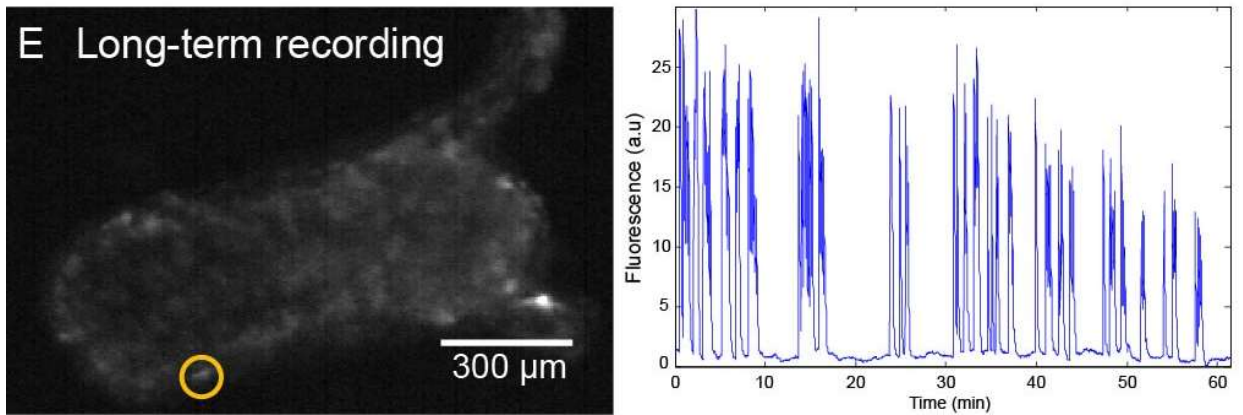


Figure 4: Imaging the entire nervous system activity of *Hydra*

A. To create the transgenic line, we injected into fertilized *Hydra* eggs (left) a plasmid that causes expression of GCaMP6s (right). B. Imaging preparation (left) and sample cross-section (right). C. Left: trajectory of 5 representative neurons. Middle: close-up on the trajectory of the 8 tracked neurons, showing a difference in direction of the neurons of the top layer (blue) versus the neurons of the bottom layer (red). Right: Single calcium spikes in neurons from both layers (top; see also Figure S2), with manual detection of coactivation events (bottom). D. First frame (top left), trajectory of all neurons (top right), close-up on the position of 2 representative neurons (bottom left) and fluorescence (bottom right) of all the detected neurons during a typical recording. Measurements were made on the first 20 seconds (real time, i.e. 1.6 seconds of movie time) of Movie S1. E. Entire animal (left) imaged for more than one hour at 30 frames per second, with fluorescence signal (right) coming from the cell circled in yellow. See also Figures S1, S2 and S4 and Movies S1 and S2.

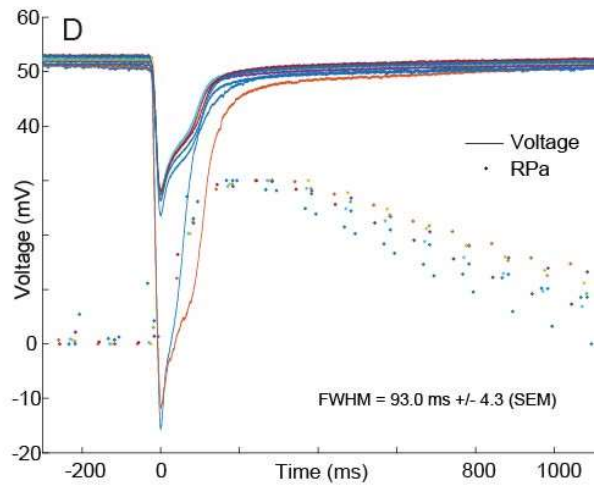
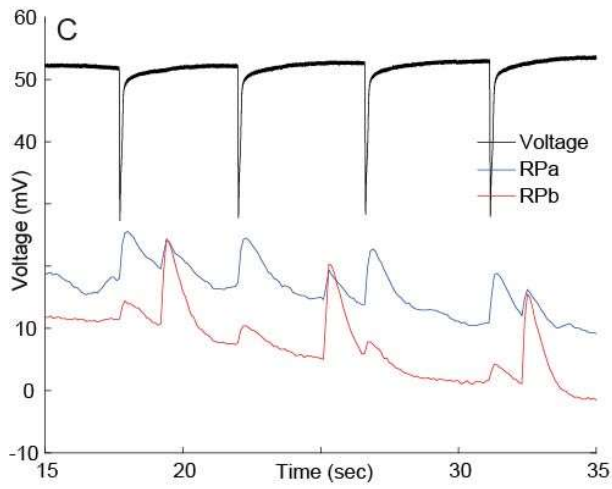
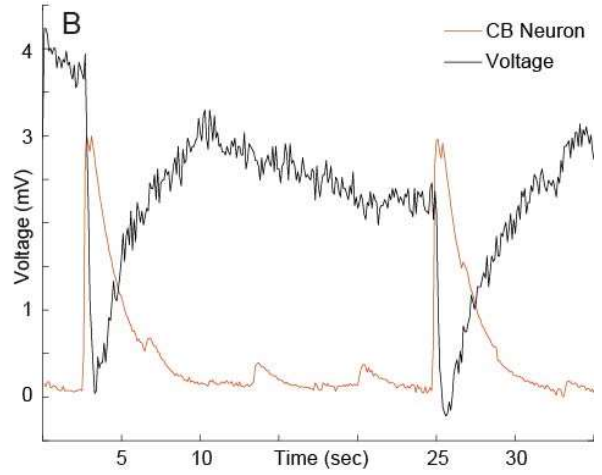
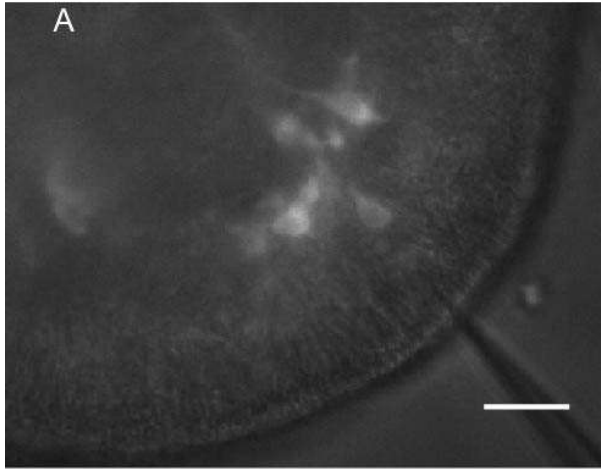


Figure 5: Simultaneous recording of electrical activity and calcium imaging

A. Preparation (scale bar = 20 μm). Electrode comes from the top and is slightly out of focus B.

Extracellular electrode placed near a contraction burst neuron, with fluorescence signal recorded from that contraction neuron. Contractions produce overwhelming electrical signal. C.

Extracellular electrode was placed close to a neuron from one RP network (RPa, which could be either RP1 or RP2) and far from a neuron from the other RP network (RPb). Accordingly, the spikes recorded in electrical activity match calcium spikes of neuron A (blue trace) but not neuron B (red trace). Note that there is cross-contamination between the fluorescence signals from neuron A and B, but one can distinguish them because of their amplitude difference (large spikes in neuron A result in small spikes in neuron B and vice-versa). D. Superimposition of nine spikes from extracellular recording and their corresponding calcium traces for neuron A. The color of each electrical trace matches the color of the corresponding fluorescence trace. In B-D, the fluorescence traces are in arbitrary units.

Functional networks of neurons in Hydra

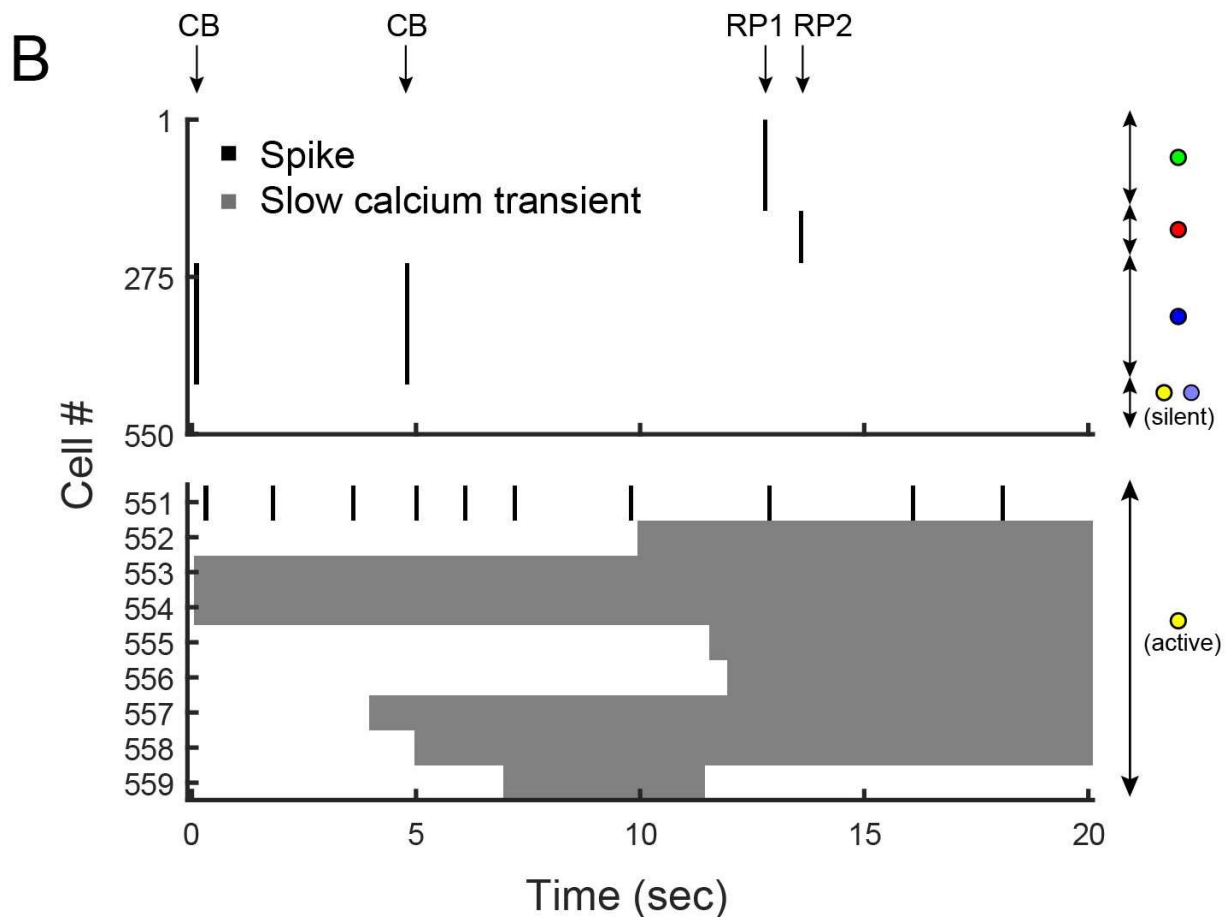
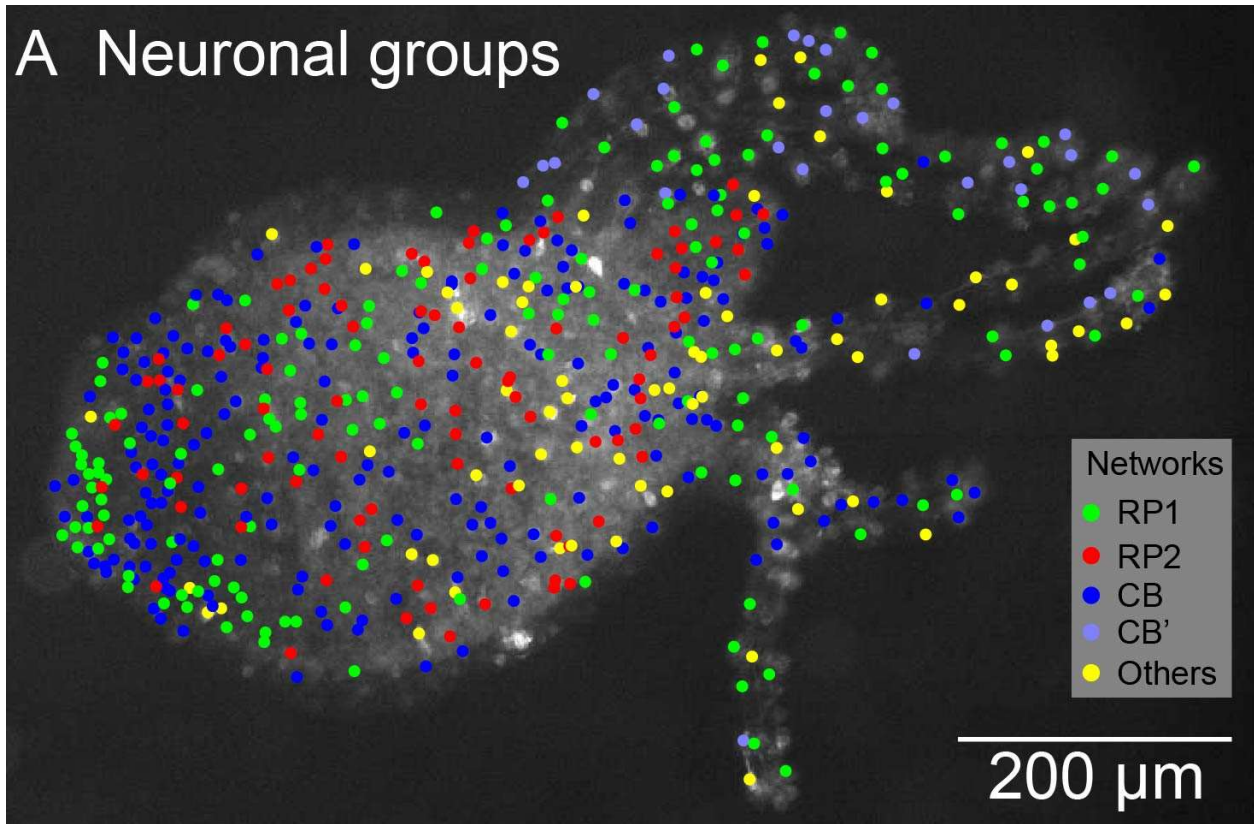
We define functional networks as groups of neurons that participate in a common function such as a particular behavior. Among these functional networks, we observed three of them where neurons spanning the entire body of the animal were coactive (Figure 6A, red, green and blue dots). Here, we define coactive as firing within the same 100ms frame (Movie S1), acknowledging that with a higher temporal resolution we might be able to measure a delay between the activation of different neurons. Interestingly, these three networks were non-overlapping, i.e. any neuron belonging to one network did not belong to any of the other two networks. Additionally, we observed small functional networks of neurons located under the tentacles-hypostome junction and individual neurons showing slower calcium transients rather than spikes (Figure 6A, yellow dots). We extracted every spike and slow calcium transients of the neurons recorded in a segment of the movie (Figure 6B). Accordingly, we reported in that segment a total of 14 activity epochs, 4 of them belonging to the coactive circuits.

One of the coactive networks involved neurons which became active during a longitudinal contraction burst (CB), which is one of the most commonly described behaviors of *Hydra* [17,37]. Such bursts happened on average once every 4.4 min (± 53 sec (SEM), $n = 6$ animals). In addition, we found networks of neurons active spontaneously, apparently corresponding to the rhythmic potentials (RPs) [17]. Unexpectedly, we found not one but two independent networks of cells generating these rhythmic potentials (Figure 6A, green and red dots), which we named RP1 and RP2 and which fired on average once every 167 sec (± 102 sec (SEM), $n = 8$ animals) and 143 sec (± 21 sec (SEM), $n = 8$ animals), respectively.

Interactions between rhythmic potentials and longitudinal contraction bursts have been described previously [3]. Since they only assumed the existence of one RP system, we explored

whether this was true for both RP networks. To examine this, we extracted the activation events of the CB, RP1 and RP2 in longer movies (up to one hour) in multiple animals and computed their cross-correlation (see Supplemental Experimental Procedures). Indeed, RP1 showed short-term interruptions when CB became active (see arrows under spike train in Figure 6C), which results in a dip at $T=0$ in the cross-correlogram between RP1 and CB (Figure 6C middle) and a decrease in RP1 frequency when CB frequency increases (cf. leftward inclination of the loops in Figure 6C right). This indicates an antagonistic interaction between RP1 and CB and was present in 7 animals (Figure 6D middle). At the same time, no detectable relationship was found between RP1 and RP2 (left) or between RP2 and CB (right).

A Neuronal groups



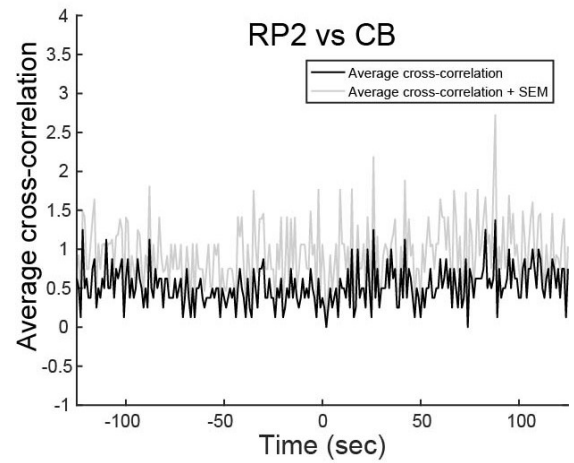
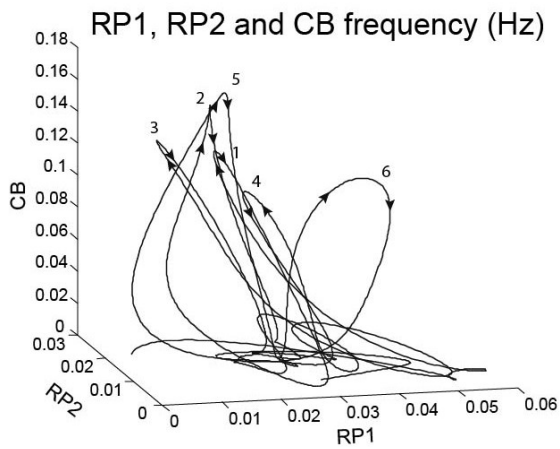
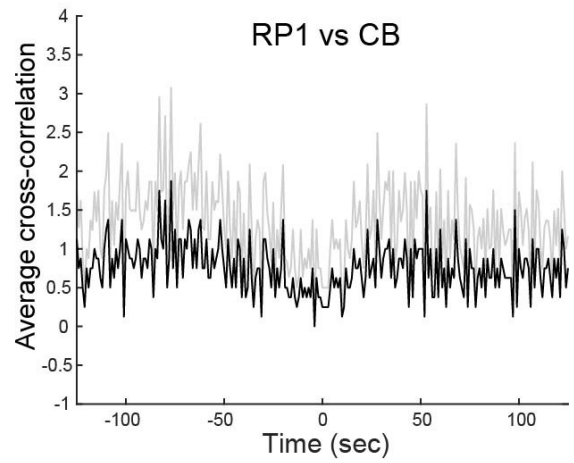
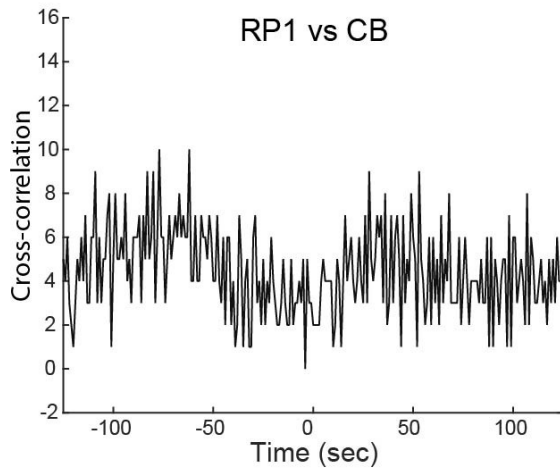
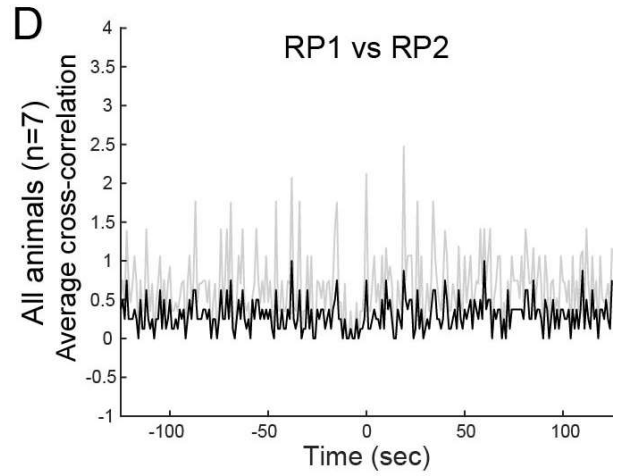
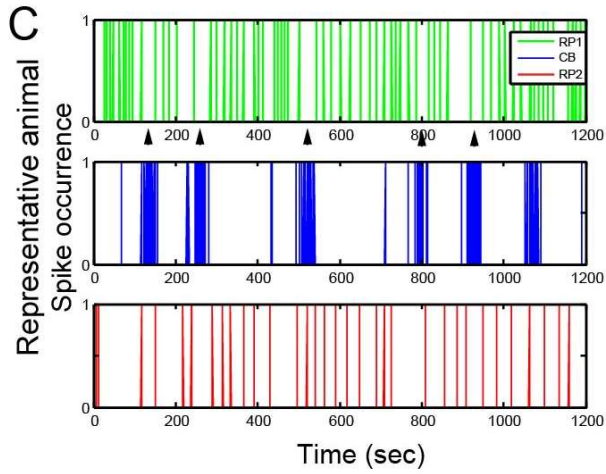


Figure 6: The nervous system of *Hydra* includes three major networks

A. Topographical distribution of neurons in *Hydra* (same dataset as Figure 4D), grouped in 5 categories: rhythmic potentials #1 (RP1, green), rhythmic potentials #2 (RP2, red), longitudinal contraction bursts (CB, blue) and other neurons (others, yellow). CB' indicates neurons of the tentacles which did not fire during the two CB events of this time window, but fired during another CB event. B. Spikes (black) and slow calcium transients (grey) of the 559 cells shown in A. Neurons are grouped by identity (colored dots on the right), and activity events are marked with an arrow (top). Note the difference in scale between the y axis of the top and bottom plots, due to the large number of neurons belonging to RP1, RP2 and CB. Also, note that the 2 activity epochs labeled as CB are the last 2 spikes of a longitudinal contraction burst. C. Top: Spiking activity of the three networks in one representative animal. Each spike represents the coactivation of the neurons of one network (RP1, RP2 or CB). Arrows indicate decrease in RP1 frequency during a longitudinal contraction burst. Middle: Cross-correlation between RP1 and CB. Bottom: plot of the firing frequency over time of the three networks. Numbers indicate longitudinal contraction bursts. D. Cumulated (over 7 animals) cross-correlation between RP1-RP2 (top), RP1-CB (middle) and RP2-CB (bottom).

RP1 and CB networks are ectodermal while RP2 is endodermal

We then examined the anatomical characteristics of the three widespread networks. Since neurons of a given network fire within the same frame (up to 30 ms in our fastest recordings) we assumed they must be connected into the same circuits either via chemical or electrical synapses. Since no neuronal connection has been described in *Hydra* between the endodermal and the ectodermal nerve net [38], we assumed that each of RP1, RP2 and CB can only exist in one nerve net (either endodermal or ectodermal). We reasoned that the CB system should be in the ectoderm because ectodermal neurons innervate the longitudinal (vertical) muscle fibers of the ectodermal skin cells in order to cause body wall longitudinal contractions. In addition, previous studies showed that the rhythmic potentials exist in the endodermal nerve net [18] and cause longitudinal contractions of the endoderm [20] which has been interpreted as producing elongation of the body column of the animal [19], because endodermal muscle cells are arranged circularly (horizontally). However, if rhythmic potentials were generated by the endodermal nerve net, they would not be able to interact with CB neurons (as shown in Figure 6D) which are in the ectoderm. Thus, we hypothesized that RP1 is in the ectoderm, which allows it to interact with CB, whereas RP2 should be in the endoderm, which prevents it from interacting with CB and RP1.

To test this hypothesis, we measured the presence of neurons belonging to the three networks in regions of our recordings that only contain the ectoderm of the animal, by taking advantage of the fact that, in our preparation, the animal is laid flat between 2 coverslips. Thus, when imaged from the objective, there is an area at the edge of the animal composed of ectoderm only, whereas the rest of the animal is a superimposition of both endoderm and ectoderm (dashed lines in Figure 7A). Accordingly, we only found RP1 neurons in areas containing ectoderm only (arrows), whereas we found RP1 and RP2 neurons in areas containing both endoderm and

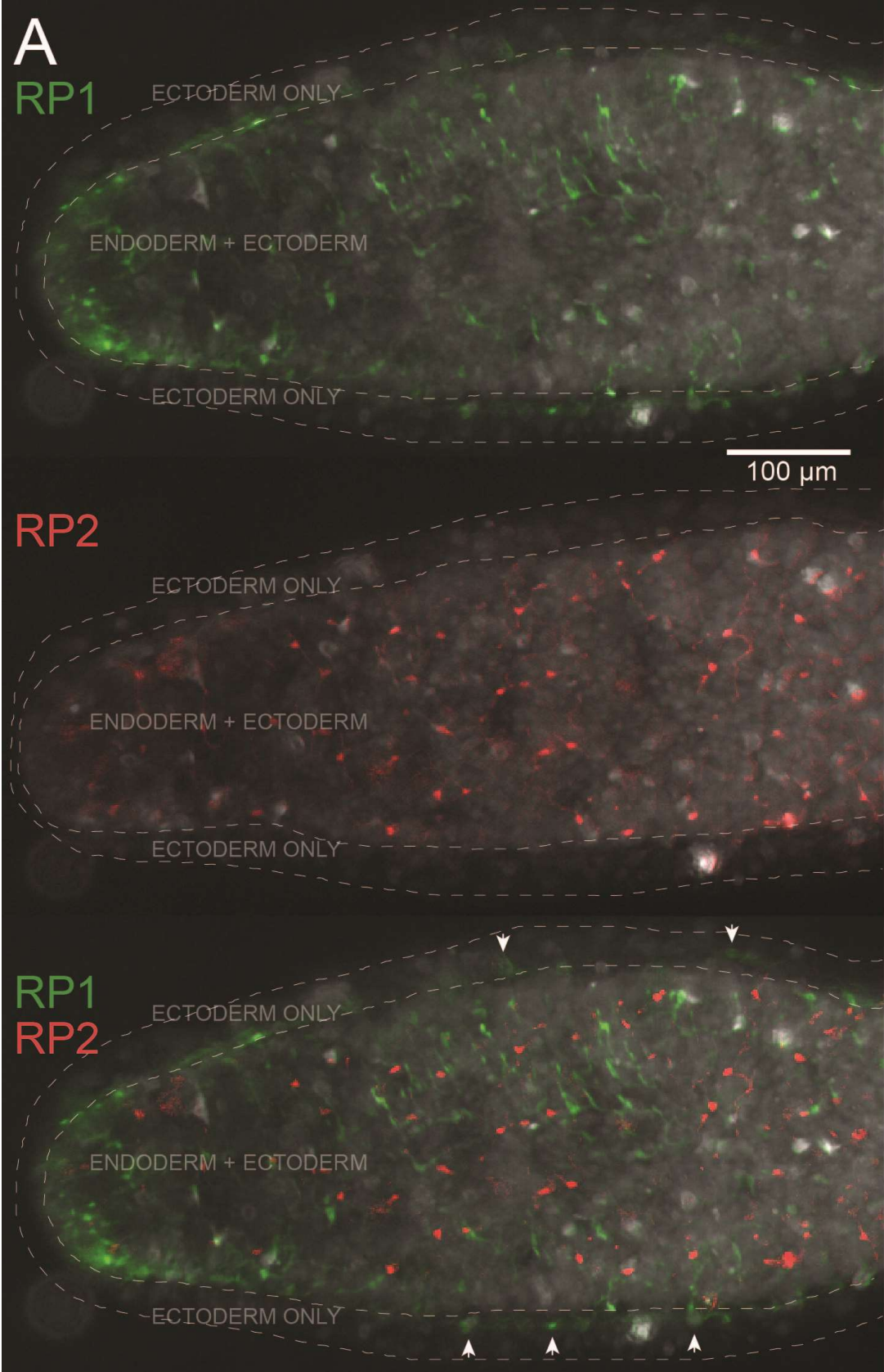
ectoderm. We concluded that RP1 is in the ectodermal nerve net whereas RP2 is in the endodermal nerve net.

We then tested whether neurons of RP1, RP2 and CB had different morphological features by comparing their soma size, number of primary neurites, and orientation of primary neurites (Figure 7B). We also measured these parameters for the individual neurons that did not participate in these three networks (“other” cells). The somata of CB neurons was larger when compared to all other categories ($10.73 \mu\text{m} \pm 0.62$ (SEM); $P < 0.01$, unpaired T-Test) (Figure 7C). Meanwhile, the number of primary neurites was higher ($P < 0.01$, unpaired T-Test) in RP2 neurons (3.2 ± 0.1) than in RP1 (2.78 ± 0.1), CB (2.9 ± 0.06) and other neurons (0.86 ± 0.2) (Figure 7D). The number of primary neurites of the other neurons was significantly smaller than all other networks ($P < 0.01$, unpaired T-Test). Some of these neurons possessed one short branch (Figure 7B), a feature that is very characteristic of the sensory neurons which have been reconstructed from serial section electron microscopy [8]. The orientation of the primary neurites was also measured (Figure 7E), by using the oral-aboral axis as a reference (top-left panel). No specific orientation was found for any of the three major networks.

To further identify the spatial structure of the three networks, we first examined the overall distribution of neurons, finding that the overall density of neurons was higher in the hypostome (3679 ± 401 neurons/mm²) than in any other part of the animal ($P < 0.05$, Paired T-test, $n=5$) and higher in the peduncle (2668.5 ± 264) than in the body column (1339.7 ± 234) ($P < 0.05$, Paired T-test, $n=5$; Figure 7F). These measurements match previous studies [14,39], where the authors dissociated specific parts of *Hydra* (hypostome, body column and peduncle) and measured the ratio between neurons and skin cells in each part. Other studies using staining methods came to similar conclusions [40–43]. Using these measurements, we calculated that CB and RP1 neurons

involved a large proportion of the neurons in the animal ($36.8\% \pm 1.87$ and 37.1 ± 1.6), as compared with RP2 (16 ± 2) and single other cells (9.93 ± 1.17) ($P < 0.05$, paired T-Test; Figure 7G). This quantification also supports that RP2 is generated by the endodermal nerve net, since previous studies [14] showed a 1/5 ratio (20%) between endodermal and ectodermal neurons, which is similar to the ratio we found (22%) between the number of neurons participating in RP2, as compared with the sum of neurons in the RP1 and CB networks (see Figure S3). Additionally, this quantification supports our earlier claim that the other neurons are probably sensory cells, since previous studies [8] also reported a very small proportion of sensory cells, as compared with ganglion cells.

Taken together, our data indicate that CB and RP1 networks are composed of two independent sets of ectodermal neurons, whereas the RP2 network is endodermal. Cells that are not part of these networks are likely to be sensory neurons.



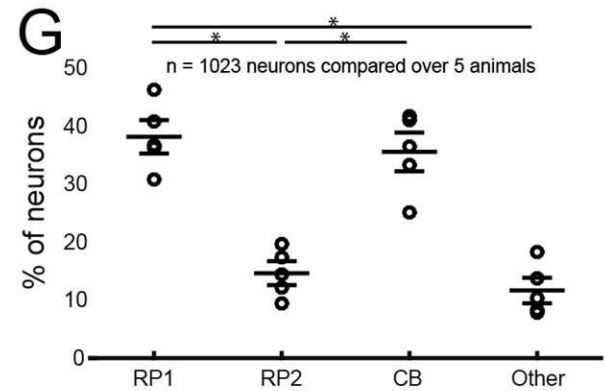
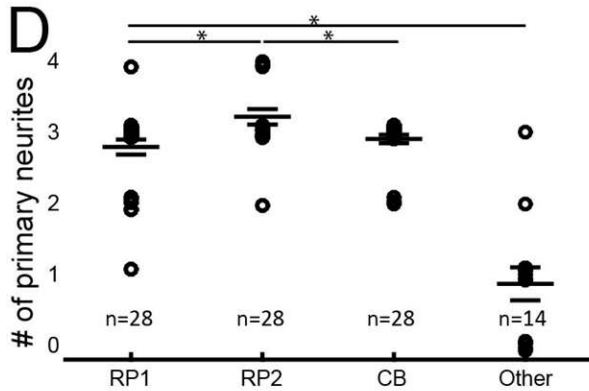
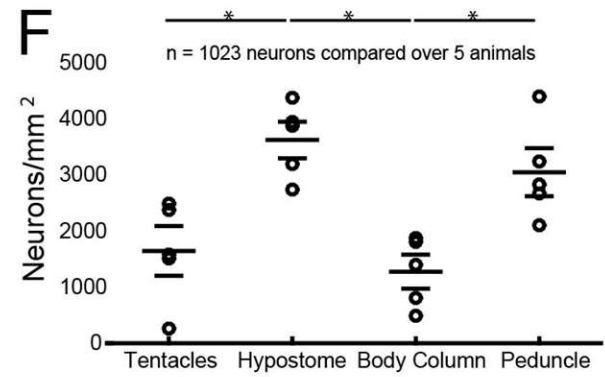
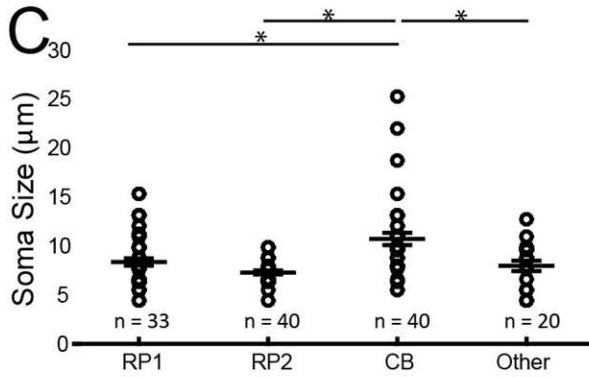
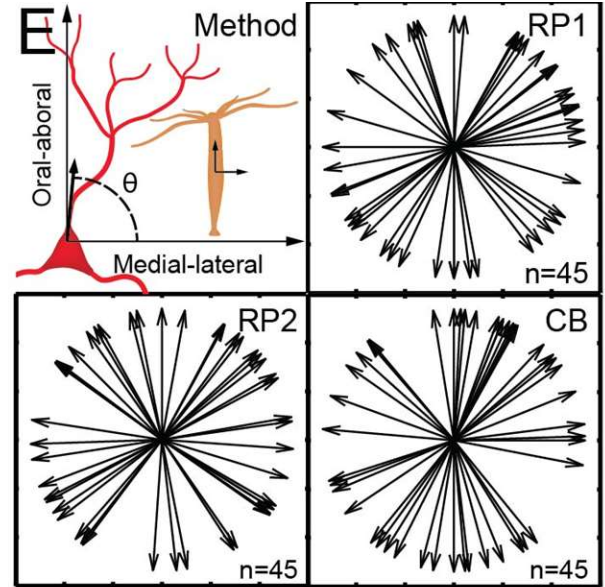
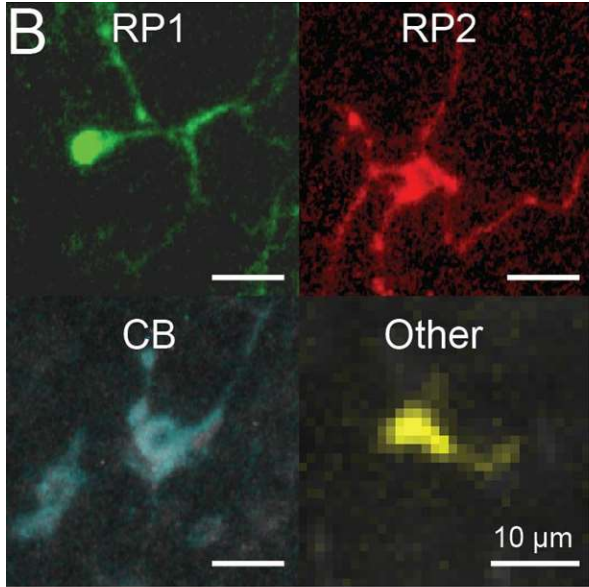


Figure 7: Anatomical differences between the three major networks

A. Pseudocolored (cf methods) RP1 and RP2 networks in an animal's body column. Top: RP1 only, middle: RP2 only, bottom: RP1 + RP2. Areas containing the ectoderm only and the endoderm + ectoderm are delineated with white dashed lines and six example neurons present in the "ectoderm only" area are marked with an arrow. B. Pseudocolored neurons representative of each of the 4 main categories. C. Soma size. D. Number of primary neurites. Note that jitter was added to the data points so that they do not overlap exactly on the plot. E. Orientation of primary neurites in neurons of the three main networks. The method to measure the angle at each neurite is described in the top-left panel. F. Neuron density in various body areas. G. Percentage of neurons belonging to each network. Data are represented as mean \pm SEM. * indicates $P < 0.05$ (unpaired T-Test). See also Figure S3.

RP1 is associated with elongations and RP2 with radial contractions

We then examined whether the activity of these non-overlapping networks correlated with any behavior. As stated, CB activity was clearly associated with the longitudinal contraction bursts of the animal. Also, as rhythmic potentials were thought to be in the endodermal nerve net, their activation should cause contraction of endodermal muscles and elongation of the body in response to a photic stimulus. For these reasons, since we found that RP1 is ectodermal, we hypothesized that the RP circuit mediating photic response was RP2. To test this we measured the activity of the nervous system of *Hydra* following photic stimulation. We induced light response by first dark-habituating animals overnight under dim infra-red light (Figure 8A). When we switched to fluorescence imaging, the light emitted by the arc lamp caused photic stimulation which resulted in elongation response (Figure 8B, where dashed lines mark contour of animal before elongation; Movie S3). To our surprise, while all three networks were mostly silent during at least 40 seconds before elongation onset, only RP1, and not RP2, became active after elongation onset (Figure 8C). Therefore, we concluded that RP1, rather than RP2, is correlated with elongations. This is in fact consistent with the fact that neurons of the tentacles are connected to photosensors [36,44] and RP2 is not present in the tentacles (Figure 6A). Also, the fact that RP1 neurons cause elongation and CB neurons cause longitudinal contraction is consistent with the anti-correlation that we observed between them (Figure 6D) and hints at a push-pull mechanism where the morphology of the animal results from a combination of the activity of two opposed neural ectodermal networks. It is important to note that, as observed previously [2], the RP1 network is also active independently of the elongation response to light, which suggests that it might be correlated with other behaviors.

We then turned our attention to the functional role of RP2. To our surprise, we discovered that radial contraction was also linked to a change in the frequency of rhythmic potentials, but that this change was specific to RP2. The slow radial contraction behavior was readily noticed in our time-lapse movies, if we played them at various speeds to recognize changes in animal morphology that happen at slower time scales (Figure 8D-E; see also Movie S4). Indeed, the frequency of RP2 *decreased* significantly after radial contraction ($P < 0.012$, paired T-Test), whereas the activity of the other networks did not change. Additionally, the frequency of RP2 was on average 10 times higher than RP1 and CB, which indicates a particularly high level of excitation before radial contraction. Therefore, we concluded that RP2 participates in radial contraction. This is consistent with the fact that RP2 is located in the endoderm (Figure 7A), and that endodermal neurons are connected to sensory cells which are exposed to the gastric environment [8]. In this context, RP2 neurons could act as an integrator of information about the gastric environment which would put them in a position to decide when radial contraction has to occur. If we consider the body column of *Hydra* as a cylinder, the relaxation of the ectodermal longitudinal fibers by RP1 during elongation would change its length whereas the activation of the endodermal circular fibers by RP2 during radial contraction would change its diameter.

Thus, we concluded that the three networks are involved in three different behaviors selectively: the longitudinal contraction bursts are correlated with the activity of CB, the elongation response to light with RP1 and the radial contraction with RP2. Thus, rather than being a single network, the nerve net of *Hydra* creates different behaviors by using anatomically separate networks of neurons.

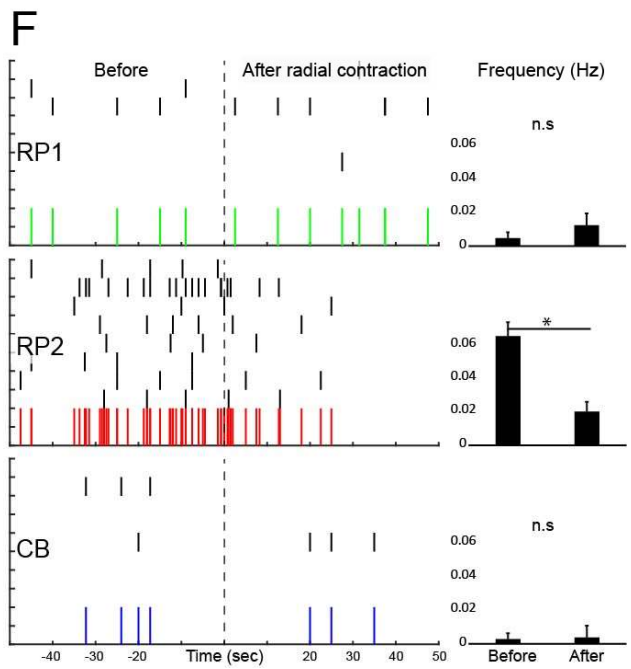
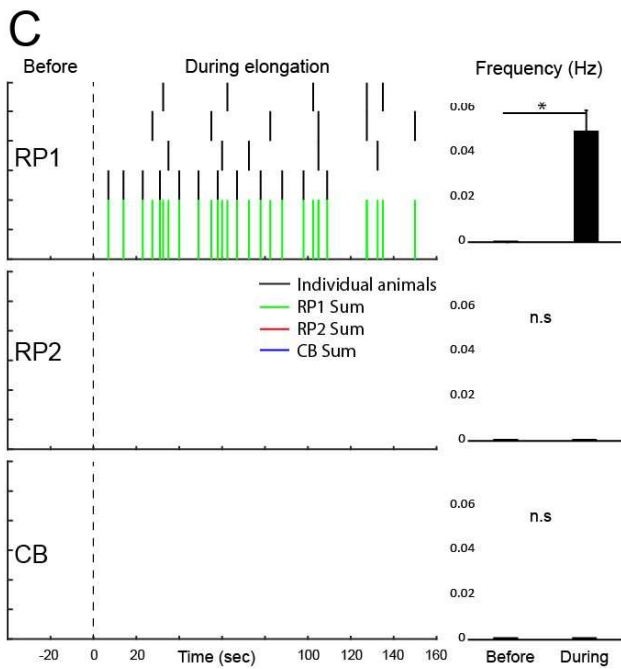
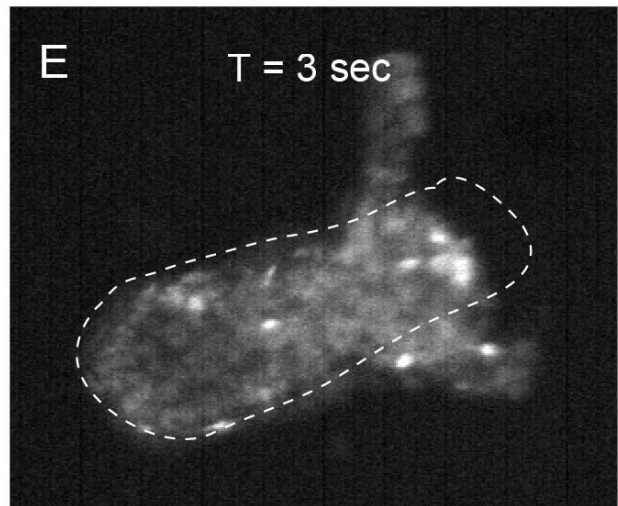
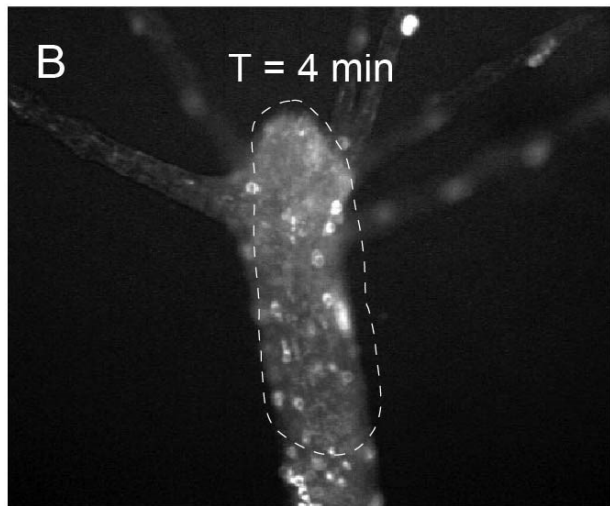
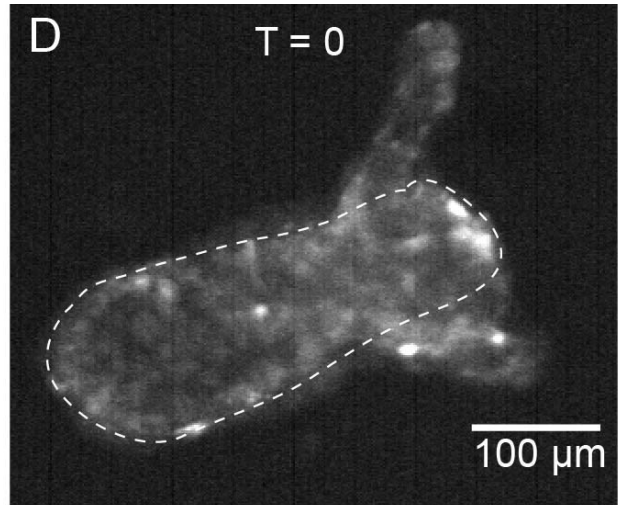
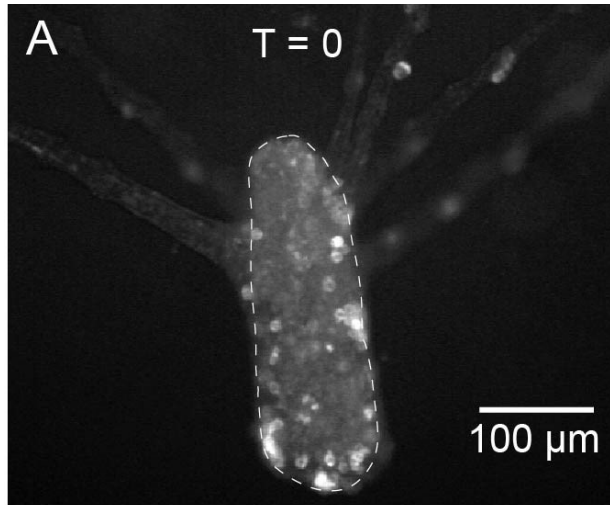


Figure 8: Behavioral association of two rhythmic potentials networks

A. Dark-habituated animal at rest. B: elongation response during exposure to blue light (see Movie S3). Dashed line marks body contour of animal at rest. C: spike trains of RP1, RP2 and CB neurons in 4 animals, where $t=0$ indicates onset of elongation. Histograms compare firing frequency before vs during elongation response. D: Animal before radial contraction, a behavior that also occurs in unrestrained preparations (Movie S5). E: animal after radial contraction (see Movie S4). Dashed line marks body contour of animal before radial contraction. F: Spike trains of RP1, RP2 and CB neurons in 8 animals, where $t=0$ indicates radial contraction. Histograms compare firing frequency before vs after radial contraction. Data are represented as mean \pm SEM. * indicates ($P < 0.05$, paired T-Test). See also Movies S3-S5.

Subtentacle network is associated with nodding

Besides the three animal-wide networks (CB, RP1 and RP2), where synchronous activation of neurons occurred throughout the body of the animal, we also observed local activation of neurons in some experiments. In particular, there was one local network that did not belong to either RP1, RP2 or CB and that was correlated with nodding behavior, i.e., gentle swaying of the hypostome of the animal and its tentacles to one side but without turning the rest of the body. This network was located just under the tentacles and we decided to call it the subtentacle network (STN). Specifically, the STN was located at the junction between the tentacle and the body column (Figure 9A). In the STN, calcium signal could propagate downward (Figure 9B) but also upward (Figure 9C). Note that in the example shown in Figure 9 neuron 1 is only activated when the signal propagates downward, which indicates that the activation of the STN circuit does not always recruit all of its neurons. The propagation speed of the calcium signal was $251 \mu\text{m}/\text{sec} \pm 54.6$ (SEM, $n=5$).

The behavioral correlation of the STN with nodding was robust: when activated, the animal always nodded (4 out of 4 animals). To quantify this, we measured the angle formed between the hypostome and the body column (Figure 9D left) as the fluorescence of the STN neurons changes and observed that the hypostome of the animal starts nodding at the same time as the neurons get activated (Figure 9D right). We did not notice any difference in nodding when the activation was upward or downward.

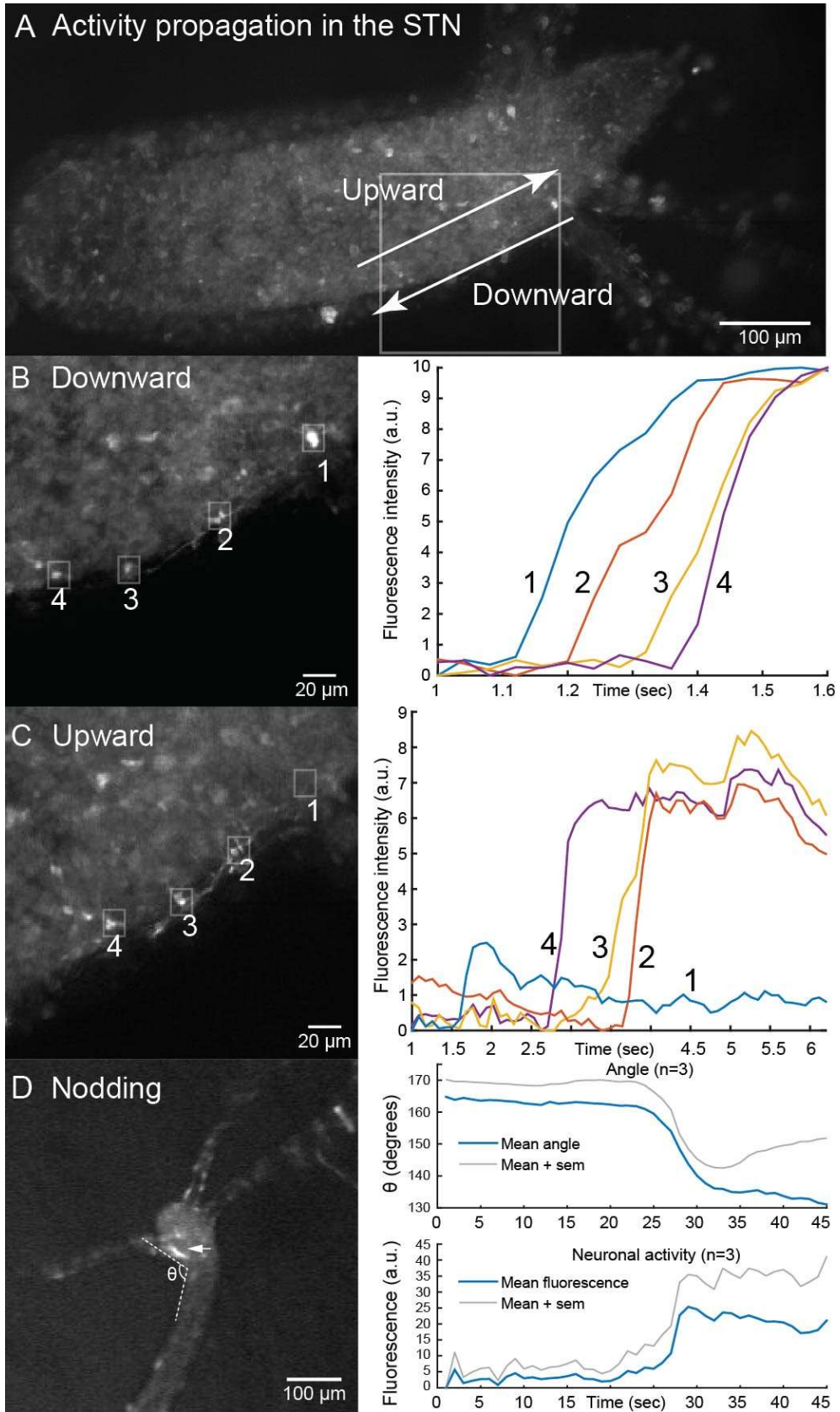


Figure 9: Subtentacle network (STN) causes nodding behavior and can conduct signal in both directions

A. Representative *Hydra*. White square marks area containing a STN. Arrows mark the two directions of propagation: upward and downward. B. Left: Region boxed in A during downward propagation, with 4 neurons marked with a white square. Right: Calcium trace of the 4 neurons during downward propagation. C. Same as B but for upward propagation. D. Left: representative *Hydra* at the end of nodding. θ marks angle, arrow marks one STN neuron. Right: evolution of angle and STN neuron activity over time.

Neuronal activity can propagate in 2 directions and at 2 different speeds in tentacles

In addition to the STN, we found another example of a local activation of neurons in the tentacles, where propagation can be bidirectional and occur at multiple propagation speeds. Specifically, in the tentacles of 4 animals we detected calcium signal which propagates slowly, enabling us to determine the exact direction of propagation of activity. We observed that activity could flow upward or downward (Figure 10A and 10B, first part of the traces) and, interestingly, in both cases slow propagation was followed by coactivation of all regions of interest (Figures 10A and 7B, second part of the traces). The average speed of the slow propagating activity was 63 ± 30 $\mu\text{m}/\text{sec}$ (SEM, $n=4$), whereas during coactivation, the speed of signal propagation could not be measured at our resolution of 33Hz (here on a field of view of 130×130 μm). This speed was therefore higher than 7 mm/sec, consistent with previous electrophysiological measurements that indicated 4.6 cm/sec [17]. However, since we cannot measure the speed of this signal propagation, it is possible that these different regions of interest are not activated in the same sequence and instead are activated in a random fashion. In all 4 observations, the neurons mediating slow propagation and coactivation were also part of the CB network, and coactivation corresponded to a longitudinal contraction burst.

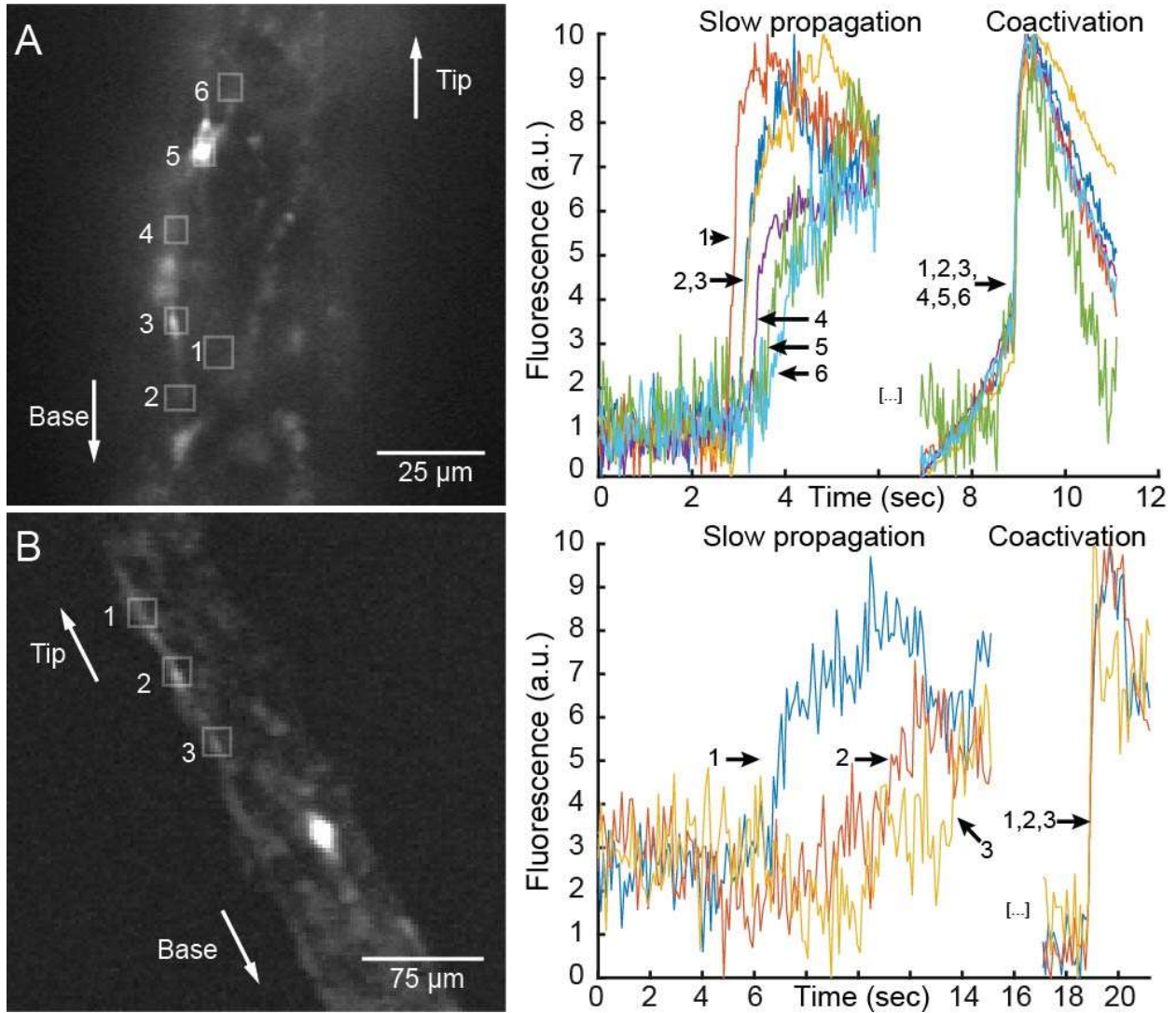


Figure 10: Signal propagates in both directions and at two different speeds in tentacles

A. Left: Representative tentacle during upward propagation, with 6 example neurons boxed and numbered in white. Right: Calcium signal of the 6 neurons during slow propagation and coactivation. B. Same as A but for downward propagation.

DISCUSSION

Hydra as a novel preparation for whole nervous system imaging

As opposed to conventional electrical circuits, the brain is made of neurons that receive and send connections to a large number of other neurons in many different regions at the same time. This organization appears ideal for the generation of emergent functional properties, built with the aggregate spatiotemporal activity of a large number of cells, and these emergent functional states, such as attractors, could be used to implement memories and many computations [45,46].

To capture these emergent states of function, it seems ideal to be able to measure “every spike from every neuron” and build a “Brain Activity Map” [47], as a step towards deciphering the role of these emergent states in the function of the nervous system or in the generation of behavior or internal brain states. In this regard, whole-brain imaging methods have been recently successful in measuring the activity of large numbers of neurons in animal models such as the worm [48–51], fruit fly [52,53] and zebrafish [54–59]. Work on these species could provide critical insights relevant to understanding the function of the nervous system of mammals and humans.

Here we introduce *Hydra* as an alternative for large-scale measurements of neural activity and to capture and investigate the emergent properties of neural systems. The choice of each animal model has pluses and minuses. While one cannot apply to *Hydra* traditional genetic tools, through the recent sequencing of its genome [28] and the development of successful transgenesis [30] one can have access to many of the modern molecular approaches standard in other fields of neuroscience. Also, as a preparation, *Hydra* offers some significant advantages for imaging entire nervous systems. Firstly, it is a cnidarian, and thus represents some of the first nervous systems in evolution, which could enable the elucidation of basic principles of neural circuits more easily. Secondly, *Hydra* can reproduce asexually by budding, enabling the generation of clonal

individuals and the examination of the structural and functional generation of a new animal. Thirdly, its nervous system is distributed without any ganglia, and the animal is transparent, so every neuron can be imaged in isolation. Fourthly, because the body of *Hydra* is flexible, it is possible to place it between two coverslips separated by 100 μm and keep the animal alive for weeks without observing any sign of injury. The behaviors we measured in this study, longitudinal contraction bursts, elongation response to light and nodding do occur in *Hydra's* natural habitat [2,3,17,21]. Because the definition of radial contraction is vague, we verified it by ourselves in an unrestrained preparation (Movie S5). However, in our restrained preparation these behaviors might be expressed in a different way. Typically, nodding and elongation response to light will only be possible on the plane that is parallel to the coverslips. Also, longitudinal and radial contractions could be somewhat slowed down because of friction of the animal against the coverslips, and the deformation of the body of the animal could be altered. To test this, we measured the duration of both types of contractions and resulting change in width of the animal (Figure S4), and did not detect any significant difference between these behaviors in an unrestrained preparation and between two coverslips.

When used with low-magnification objectives, such preparation allows having the entire network of neurons in focus and alleviates the need for scanning multiple planes in z . Therefore, it is possible to observe the activity of the entire nervous system of *Hydra* with a higher temporal resolution while keeping a spatial resolution of single neurons. These advantages make it easier to measure single calcium transients in a behaving animal and attribute them correctly to the neurons that generated them, getting to the ideal of measuring every spike from every neuron [47]. In fact, using immunocytochemistry we estimate that we are indeed recording the activity of essentially

every neuron in the animal. Moreover, at least for many neurons, we are likely also imaging individual calcium transients.

As an animal model for circuit neuroscience, *Hydra* is amenable for imaging and offers a small repertoire of behaviors to study. We presented the activity of the nervous system during longitudinal contraction bursts, elongation response to light, radial contraction and nodding, but other behaviors exist such as somersaulting and feeding. Both of these behaviors add another layer of complexity, because they happen in multiple steps which require coordination of activity across the entire animal. For instance, feeding behavior engages first a concerted motion of the tentacles, after which the prey is brought to the mouth in order to be swallowed and digested through peristaltic motion of the body column. Therefore, imaging *Hydra* during these behaviors would help exploring coordination of activity across different parts of its nervous system.

Nonoverlapping coactive networks of neurons in the nerve nets of Hydra

Using calcium imaging, we perform the first functional measurements of neurons in *Hydra* and can associate previously recorded electrical signal such as RPs and CBs to specific populations of neurons. Also, a striking feature of the RP1, RP2 and CB networks is the fact that their neurons are coactive (they fire simultaneously or at least within 100ms). We are still ignorant about the exact connectivity of these neurons, and the joint activity could be the result of either gap junctions connecting every neuron, strong chemical synapses that have a very low failure rate, or inputs from another circuit that is connected to every neuron of this network. Indeed, both chemical synapses and gap junctions have been found in *Hydra* [4,5], but a third circuit mediating coactivation seems less likely since we do not observe activity of any other circuit that is simultaneous to RP1, RP2 or CB.

But regardless of the exact mechanisms of coactivation, we have discovered that the nervous system of *Hydra* is divided into networks that are non-overlapping structurally and functionally, i.e., where individual neurons participate selectively in specific networks and no neuron belongs to more than one network. Moreover, these networks (CB, RP1, RP2 and STN) are associated with specific behaviors of the animal (longitudinal contractions, elongation, radial contraction, and nodding, respectively). As mentioned above, most neurotransmitters can be found in the *Hydra* genome, so there could be a molecular identification to the networks of neurons we identified functionally.

The finding of non-overlapping networks indicates that the nervous system of *Hydra*, and perhaps other cnidarians, is not a single nerve net but is built out of distinct networks which activity can be linked to specific behaviors. Thus, evolution has carved out a behavioral repertoire by selectively linking subsets of neurons out of a tapestry of apparently similar cells, since each subset of neurons is associated with a specific behavior. This carving could occur by selectively connecting neurons into subcircuits, or by modifying synaptic strengths. Future work combining connectomics with functional imaging could examine these mechanisms of functional specificity.

Two rhythmic potentials networks

The use of whole-brain calcium imaging has also allowed us to identify two networks associated with the rhythmic potentials, previously described using extracellular recordings [3]. These two networks (RP1 and RP2) are located in the ectoderm and endoderm of the animal respectively. A previous study reported that rhythmic potentials are only generated in the endoderm [18] by showing their absence in an area where the endoderm had been surgically removed. However, in that study the authors reported having recorded in rare instances rhythmic potentials in the ectoderm but they attributed this signal to an incomplete removal of the endoderm

in the recorded region. According to our present results it is likely that in most cases the authors recorded the endodermal RP2 signal and in rare instances they recorded the ectodermal RP1 signal. Also, our report that contraction of the endoderm causes radial contraction is in apparent contradiction with the report that rhythmic potentials could cause contraction of the endoderm [20]. Indeed, since a change in the frequency of rhythmic potentials was observed during elongation response [2], it was concluded that contraction of endodermal cells would cause elongation of the animal. However, based on our data, we suggest that the contractions observed by [20] originated in the endodermal RP2 system which is correlated with radial contraction, whereas the response to light in [2] arose from the ectodermal RP1 which is correlated with elongation.

Interestingly, although RP1 and RP2 are associated with elongation and radial contraction, respectively, since changes in their frequency of activation were clearly associated with behavior, there was no clear cut temporal correspondence between the activity of RP1 and elongation or between the activation of RP2 and radial contraction (Figure 8). Thus, we hypothesize that, rather than directly triggering or controlling behavior, these two rhythmic potential networks may integrate sensory information which then subsequently triggers the behavioral response, through a different cellular element, perhaps even through epithelial cells.

Bidirectional propagation in the subtentacle network

Slow potentials that occur simultaneously to asymmetric longitudinal contraction of the body column were reported in [2]. However, in their experiments it was not possible to prove or exclude the participation of neurons. Here, we describe the activity of a specific network of neurons (the STN) that are located under the base of the tentacles and which are activated during such behavior.

The sequence of activation of the STN can either initiate in the body column and travel towards the tentacles, or initiate in the tentacle-hypostome junction and travel downward. This flexibility could have a role, such as fine-tuning the resulting motor output by changing which part of the body should bend first. Also, it may have no specific function but arise from the fact that the STN can be activated by different neurons. Indeed, it is possible that activity in the body column and in the hypostome can initiate STN activity. Then, depending on which one happens, the STN will start either at the hypostome-tentacle junction or in the body column.

Multiple conduction speeds

The existence of multiple conduction speeds within the same network has been described in other hydrozoans such as *Aequorea* [24] (p.482) and anthozoans such as *Calliactis* [60]. For instance, in the hydrozoan *Aequorea*, the radial conduction system is slow (0.002-0.02 m/sec, i.e. 2-20 mm/sec) whereas the swimming beat system is much faster (0.9 m/sec). In our experiments, we observed that in the tentacles of *Hydra* there are calcium transients that travel at $63 \pm 30 \mu\text{m}/\text{sec}$ (SEM, n=4) and others that might travel at more than 7 mm/sec which differs by two orders of magnitude. As mentioned above, the neurons where slow and fast propagation was observed are part of CB and it is only during fast propagation that longitudinal contraction occurred. Therefore,

slow propagation could be the result of a different type of activity that is initiated in one neuron and travels to its neighbors. Such activity could increase the excitability of ganglion and sensory neurons, but could even affect the sensory structures such as nematocytes to which they are connected. In this regard, measuring calcium transients in nematocytes would provide valuable information to study their interactions with neurons.

Broader relevance to neuroscience

The findings presented here may extend to understand the structure and function of the nervous systems of other cnidarians and basal metazoans. The electrical activity and behaviors of other polyps and medusae has been studied before [24] and many similarities are shared among animals of this phylum. Such similarities include the existence of nerve nets, the spontaneous longitudinal contractions and the characteristic sequence in feeding behavior. Accordingly, the presence of two networks in the ectodermal nerve net and one network in the endodermal nerve net could be a general feature of the polyp form of cnidarians. From a different perspective one could take advantage of the subtle differences between polyps of different species, which change in size, shape and in the type of prey they feed on. In such comparative studies, one could test the role of a specific feature on the anatomy, electrical activity and behavior, in an animal where most of the other parameters are essentially the same.

In addition to the interest in the neurobiology of basal metazoans, studies on the nervous system of *Hydra* could have relevance to understand neural circuits in bilaterian species. Indeed, coordinated spontaneous activity, robustly present in *Hydra*, is common to all nervous systems observed, including visual cortex [61] and human EEGs. Additionally, it has been proposed that brain waves have evolved from an early form of spontaneous activity such as the one observed in

Hydra [62]. Also, our finding that the activity of the endodermal nerve net is correlated with the activity of the gastric cavity (radial contraction, Figure 8B) is reminiscent of the enteric nervous system controlling the gastro-intestinal tract of higher animals. More generally, the study of simpler organisms could enable to discern some basic principles such as emergent properties of neural circuits, analyze the anatomical, biophysical and synaptic mechanisms that generate them, and understand how they relate to behavior or internal brain states.

GRASS FELLOWSHIP PROJECT – ARC CYCLES

Introduction

The two different types of contractions that have been presented in this work can occur both in unrestrained and in restrained animals. We have shown that they are correlated with the activity of specific circuits in the nervous system of *Hydra*, and that their execution can be influenced by various stimuli such as light and touch. One missing piece of information relates to how frequently these behaviors occur, and whether there is an pattern in the display of these behaviors. Most animals follow cycles, which can be related to the presence of food or simply the circadian alternation of day and night. In this project, I attempted at testing whether such cycles exist in *Hydra* simply by measuring the occurrence of both contractile behaviors over long periods of time.

Method

The simplest way to measure the occurrence of a behavior is to measure a parameter that is related to it. Fortunately, the thickness of the animal is a good correlate for both types of contractions since it will change drastically during their occurrence. Indeed, during longitudinal contractions the reduction in length of the animal causes tissue squeezing in the middle of the body column

which makes it enlarge especially in the middle of the animal. During a radial contraction though, the thickness will abruptly decrease since the diameter of the body column is reduced.

An algorithm called local thickness is available in Fiji [63] which measures the thickness of an object over the duration of a movie. Some image preprocessing is necessary in order to gather a sufficient signal-to-noise ratio and enables the algorithm to detect the object. Fortunately, in our case the operation contrast enhancement is most of the time good enough.

Once the preprocessing is done, the algorithm can be run and the output looks like in Figure 11. Changes in the animal thickness can be seen as spikes and ramps on the right part of Figure 11, which plots the average thickness at each time point over the whole duration of a movie. Spikes correspond to longitudinal contraction bursts and ramps correspond to radial contractions.

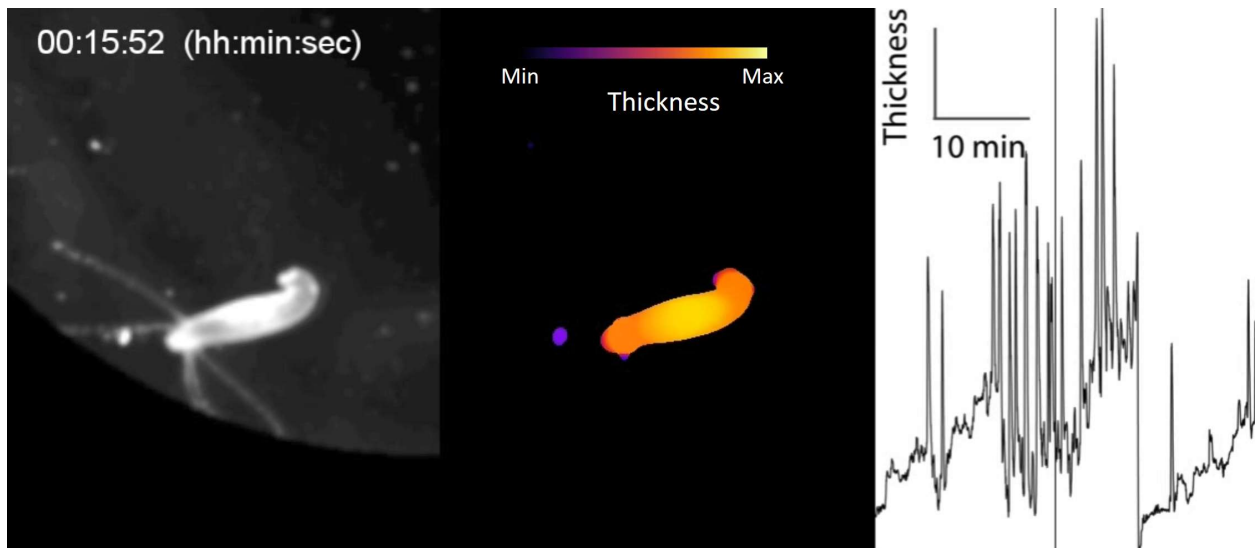


Figure 11: Thickness measurement

(Left) Raw movie. (Middle) Output of the algorithm. (Right) Average thickness in each frame over the whole movie, with the vertical bar indicating the time point that corresponds to the frames shown in the middle and on the left.

The next step in the procedure is to use the changes in animal thickness in order to detect both behaviors (radial and longitudinal contractions). This can be done using an algorithm in MATLAB that will read the progression of the animal's thickness over the movie and detect both spikes and ramps. Ramps are more challenging to detect and in order to do so I used a method called sliding window. For each time point, the sliding window measures the average thickness over the previous 15 minutes and subtracts it from the average thickness of the following 15 minutes as shown in Figure 12. As a result, the maximum value of the sliding window will be at the end of the ramp, which is precisely when a radial contraction occurs.

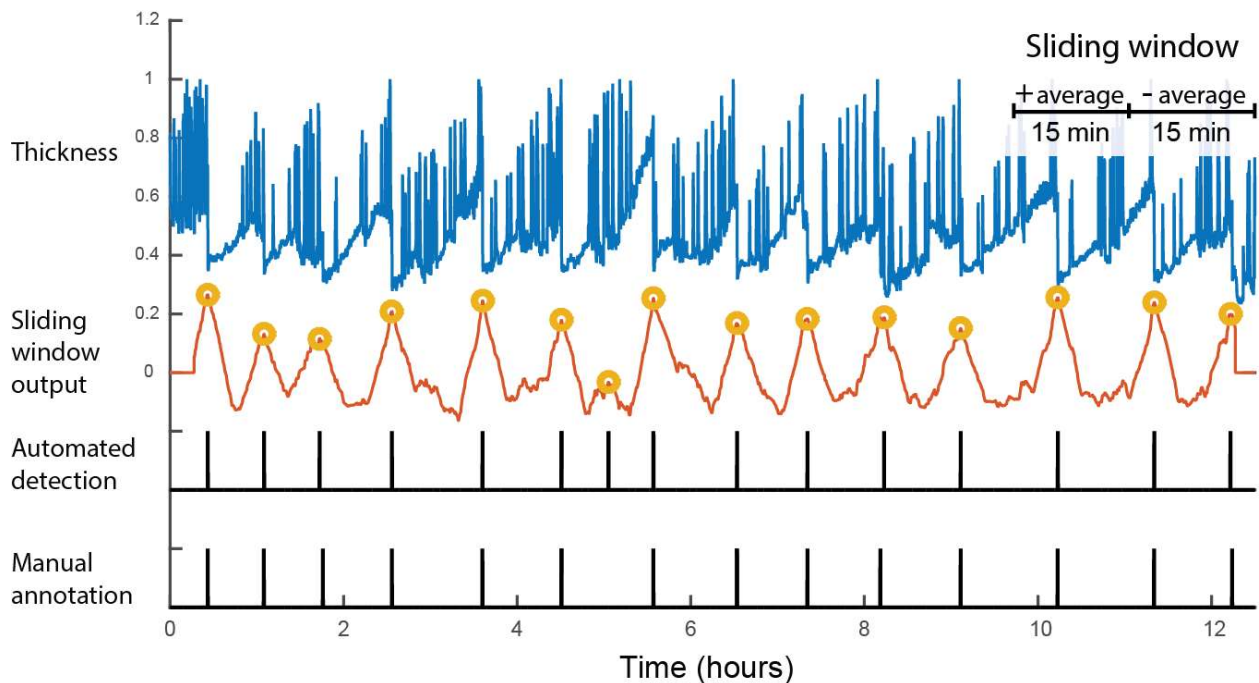


Figure 12: Detection of radial contractions

By using a sliding window which measures for each time point the difference between the average thickness of the past 15 minutes and the average thickness of the following 15 minutes, one can find the time point at which a ramp ends. Top row: average thickness over time. 2nd row: output of the sliding window. 3rd row: automated detection of the radial contraction behavior, simply done

by marking the maxima of the 2nd row. 4th row: manual detection of radial contractions done by just watching the movie. Accordingly, in this example, one mistake was made by the algorithm out of 14 events.

It is easier to detect longitudinal contraction bursts as they show up as spikes in the thickness measurements. Therefore, with MATLAB one can simply use the function *findpeaks* in order to mark the events of longitudinal contractions as shown in Figure 13.

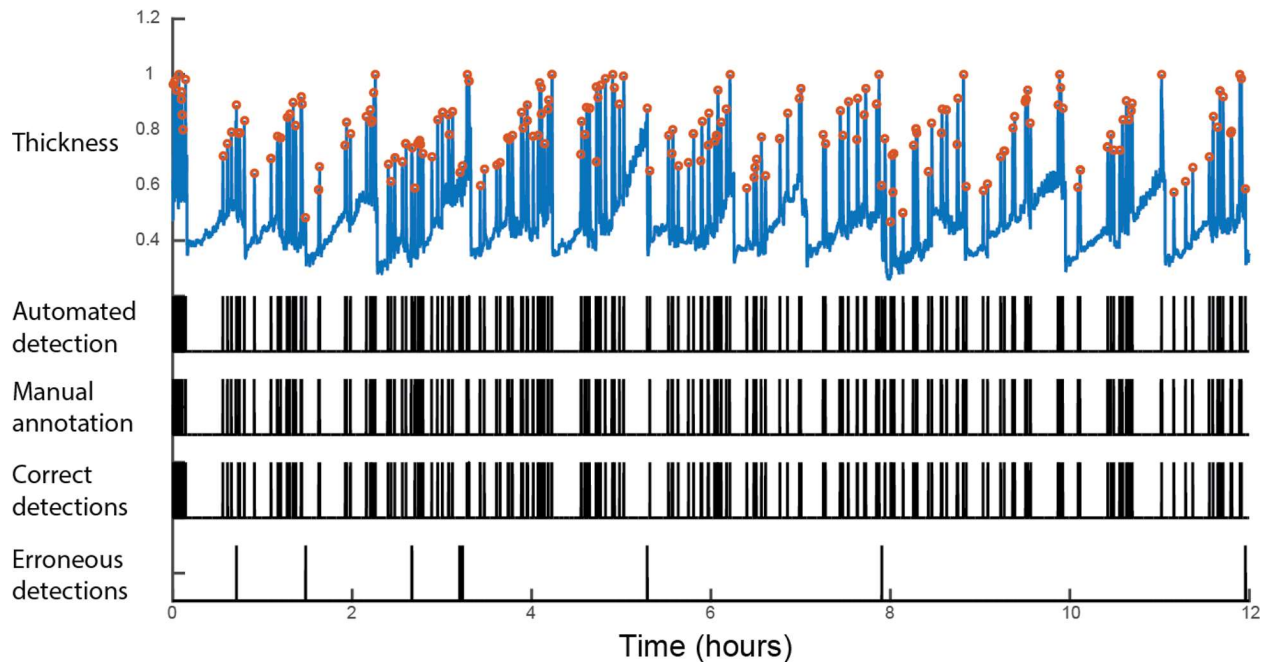


Figure 13: Detection of longitudinal contractions

Top row: thickness measurement. 2nd row: detection of longitudinal contractions using *findpeaks*. 3rd row: manual detection, done by simply watching the movie. 4th row: correct detections, i.e. detections made by the algorithm which match the manual detections. 5th row: erroneous detections, i.e. detections missed by the algorithm and detections made by the algorithm which do not match the manual detection. Accordingly, in this example again the percentage of erroneous detections is below 10% of the events detected manually.

As a result, such algorithm detects with about 90% accuracy the occurrence of longitudinal contractions, which is a performance that is similar to the detection of radial contractions shown above. With such a tool one can now measure the occurrence of both types of contractions for an arbitrary amount of time since it can be done automatically. This should help searching for temporal patterns in the behavior of *Hydra* such as sleep and circadian cycles, which is the goal that was proposed for this project.

Results

When displaying the average thickness of an animal over multiple days, one can look for patterns in the behavior. To look for circadian cycles, one can separate such recording in 12 hours time windows (9am to 9pm and vice-versa) which corresponds to day and night, i.e. when the animal was exposed to the daylight or in the dark. When doing so, I was not able to observe any obvious change in the frequency of longitudinal and radial contractions when comparing day versus night (Figure 14). However, it appeared that the ramps that end with a radial contraction always followed each other, without any interval. Indeed, it seems like the animal is always in the process of intaking water and therefore swelling, until a certain point where a radial contraction is triggered thereby expelling that water. I decided to describe these as absorption-radial contraction cycles, or simply ARC cycles, and to use them as an elementary unit to describe the temporal structure in the behavior of *Hydra*.

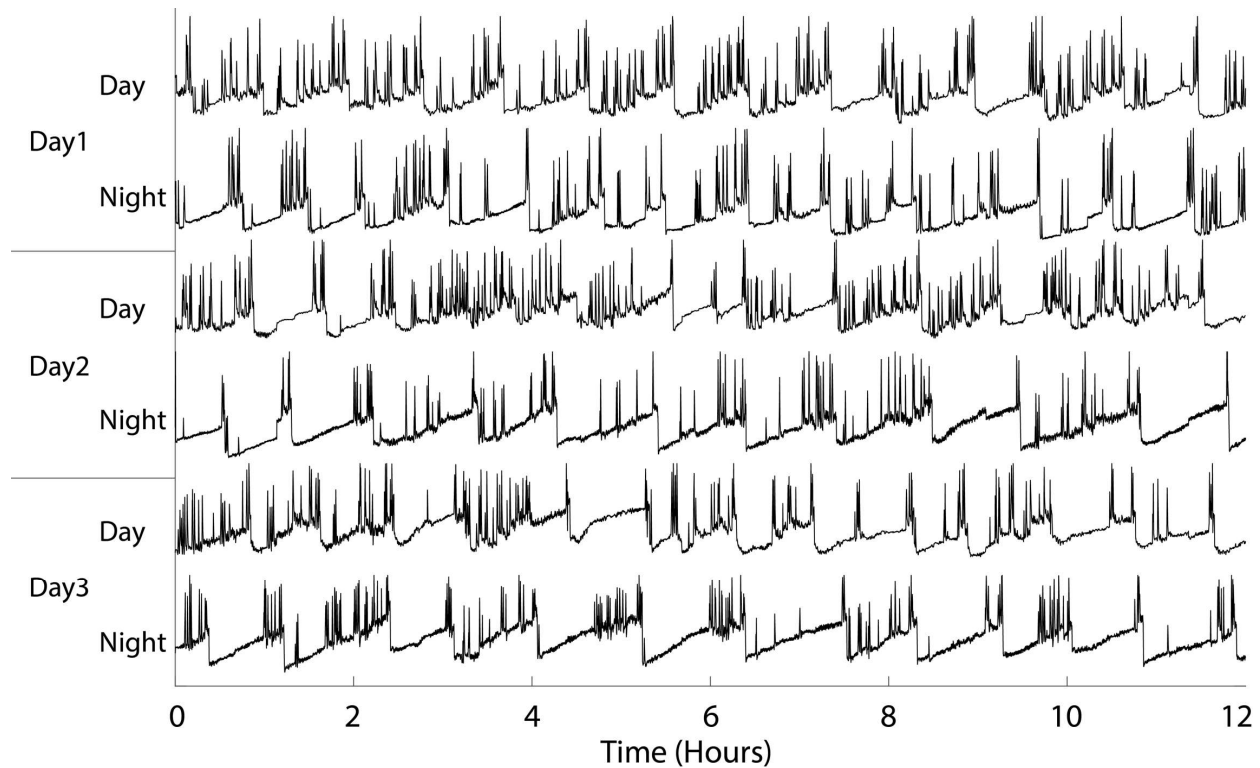


Figure 14: Continuous thickness measurement over 3 days

I used the algorithm presented above to measure the thickness of an animal over 3 days and detect changes in the occurrence of both types of contractions. Each day is separated between the daytime and the nighttime. Although there is no apparent difference in the activity during the day versus the night, a simple type of temporal structure is apparent: the ramps that constitute an absorption of medium followed by a radial contraction of the animal (ARC) succeed each other without any interval. By definition, this constitutes a cycle which we can refer to as ARC cycle.

Discussion

Temporal structure in the behavior of an animal can help inform about its intentions and how its decisions are made.

Here, I have presented a method to automatically detect the occurrence of two behaviors in *Hydra* which are fundamental within the behavioral repertoire of the animal: longitudinal and radial contractions. Both of these behaviors can be expressed in the absence of an external stimulus, but can also be triggered by touch (for longitudinal contractions) and feeding (for radial contractions). With this method I could observe that both behaviors can indeed be expressed by the animal in the absence of any external stimulus, but more surprisingly this happens over periods of multiple days in a constant environment. Such constant environment is in fact the same preparation as was used for calcium imaging in published work [64], i.e. confinement between two coverslips separated by a 100 μ m spacer.

This method enabled to observe that the animal continuously absorbs medium which causes swelling, and every so often expels that medium through a radial contraction. Because there is no interruption in the process of medium absorption, each ramp ends with the beginning of the next one, hereby forming absorption-radial contraction (ARC) cycles. Such cycles can be considered as an elementary temporal unit and be used to test the effect of various perturbations such as a change in osmolarity (which should change the process of medium absorption) on the behavior of the animal.

In the future, considering that we have been able to record the behavior of *Hydra* over long periods of time, it would be useful to record the activity of its nervous system for these prolonged periods of time. Since one can observe cycles in the behavior of the animal, it is very likely that one can observe cycles in the activity of its nervous system as well.

However, as well as it was necessary to develop a method for automatically detecting behaviors in *Hydra* over long periods of time, it will also be necessary to develop algorithms to detect

activity in the nervous system of *Hydra* over long periods of time. Such algorithms could use machine vision in order to track all the neurons while the animal is moving.

CONCLUSION AND FUTURE DIRECTIONS

In this work we have seen that the nervous system of *Hydra* is amenable for calcium imaging mostly because this animal is transparent and its neurons are spaced rather than clustered. This gives the convenience of a high signal-to-noise ratio and the possibility to distinguish between every neuron, i.e. have single neuron resolution. Thanks to these properties it has been possible to observe the activity of the entire nervous system of *Hydra* while the animal was behaving, and subsequently associate circuits with specific behaviors.

Conserved features in the nerve net

In the phylum of cnidarians, there are other animal models for which transgenic manipulations are possible. For instance, *Hydractinia* and *Nematostella* have been used repetitively to create lines expressing a transgene (Figure 15). This means that it might be possible in the future to test whether what we have learned in *Hydra* is also valid in other cnidarians. For instance, do we also have 3 large groups of coactive neurons in these other animals? If yes, do they fulfill the same roles, and do they use the same molecules in order to fulfill these roles? Do they possess the same types of synapse?

If one can perform calcium imaging in *Hydra*, one can certainly perform calcium imaging in *Hydractinia* and *Nematostella*. However, the quality of the recordings might not be the same. Indeed, in the case of *Hydractinia*, the thickness of the animal is going to be significantly higher

than in *Hydra*, since this is a colonial hydrozoan and multiple animals are stuck together. In the case of *Nematostella*, there are pigments in the epithelium of the animal which will attenuate the fluorescence light and therefore reduce the signal to noise ratio.

Also, when it comes to comparing the nervous system of multiple animals, one major difference between *Hydra* and these two other species of cnidarians is that *Hydra* lives in freshwater, whereas both *Hydractinia* and *Nematostella* live in salt water. This will unavoidably have major consequences on the ion channels that they express on the surface of their cells in order to establish the right intracellular ion concentrations. Still, one would expect that this transition can be made while keeping the various functions of the nervous system.

Hopefully, these experiments will turn out to be pretty straightforward and one will be able to tell to what extent the nervous system of *Hydra* is stereotypical of the nervous system of cnidarians. The parameters that are the same could then represent fundamental organizational principles of the nervous system.



Figure 15: Other cnidarians have transgenic capabilities

Left: *Hydractinia* (credit: nicotralab.org). Right: *Nematostella* (credit: thomsenlab.org). These animals could turn out to be very useful to test whether what we have learned from *Hydra* also applies to other nerve nets.

EXPERIMENTAL PROCEDURES

Hydra maintenance

Hydra were maintained in the dark at 18C and were fed freshly hatched *Artemia* nauplii once a week or more frequently when necessary.

Transgenics

Transgenic lines were created according to Juliano et al, 2014 using a modified version of the pHyVec1 plasmid (Addgene cat#34789) [34] where we replaced the GFP sequence with a GCaMP6s sequence that was codon-optimized for *Hydra* (DNA2.0, Menlo Park, CA). By embryo microinjection one gets mosaic animals, where ectoderm, endoderm and interstitial lineages can become transgenic separately [65]. We selected animals only expressing GCaMP6s in the interstitial cell lineage. Also, interstitial cell lineage includes neurons, cnidocytes and gland cells. However, it was possible to discriminate them from neurons in our movies because of their morphological features (only neurons have neurites).

Imaging

In order to record the activity of the nervous system of *Hydra*, we developed a new preparation for functional imaging. Animals were placed between two coverslips that are separated by one 100um spacer to keep them on focus. In this preparation, animals might not behave as they would in their natural habitat. However, it makes it convenient to look at the activity of the nervous system of *Hydra* during specific behaviors. Imaging was performed using a fluorescence dissecting microscope (Leica M165) equipped with a long-pass GFP filter set (Leica filter set ET GFP M205FA/M165FC), a 1.6x Planapo objective and a sCMOS camera (Hamamatsu ORCA-Flash 4.0) or an Olympus IX-70 inverted microscope equipped with 10x water immersion objective, a U-MIWIB2 GFP filter cube and an EM-CCD (Hamamatsu EM-CCD C9100-12). In

both setups, illumination came from a mercury arc lamp and the software micromanager [66] controlled the microscope. Single neurons were tracked manually, frame by frame, using the graphic user interface of TrackMate [63] and no automated tracking algorithm was ever used (Movie S2). Such single neuron tracking was only performed to generate Figure 4D and 6B and show that the three circuits of neurons (RP1, RP2 and CB) are mutually exclusive. When a neuron was particularly challenging to track (cf blue circle in Figure 4D bottom left), visual landmarks from the surrounding tissue were used as guiding points. For the rest of the manuscript, we only measured at which frame these (RP1, RP2 and CB) networks of neurons fire, which we call “coactivation events” (Figure 4C (right)). This is much more straightforward to measure for two reasons. First, whenever any of these circuits is activated, a larger number of neurons fire during the same frame which makes it easy to detect. Second, each circuit is easily recognizable: activation of CB always results in longitudinal contraction and RP1 but not RP2 invades the tentacles. Data coming from these measurements was then plotted as a spike train (Figure 4C (right, green bars), Figure 6 and Figure 8), where each spike indicates coactivation of all the neurons of that circuit. All the collected data was handled with MATLAB (The Mathworks, Natick, MA). The main advantage of this preparation is the fact that there is no need to scan in the z axis, and therefore the acquisition speed is only limited by the camera. The main disadvantage is the fact that by using widefield imaging rather than confocal or 2-photon imaging, the spatial resolution is worse (about $1\mu\text{m}$ for widefield when compared to less than $0.4\mu\text{m}$ for the others). This can result in cross-contamination between regions of interest, and for instance increase in fluorescence of some RP1 neurons during a CB event because of light scattering coming from CB neurons lying in close proximity of the recorded RP1 neuron (e.g. in Figure 5C). This cross-contamination makes it difficult to tell whether a neuron is firing based on

fluorescence trace alone. However, it is easy to tell in movies when a neuron is firing because its neurites are also lighting up. For this reason, the spike times were manually measured in the movies for each neuron.

Pseudocoloring

We used pseudocoloring as a method for identifying neurons that fired during the same frame (e.g. in Figure 7A). For a given firing event, using ImageJ [67] we subtracted the frame before neurons fired from the frame during which neurons fired. We then added the result of this subtraction in a specific color to the frame before neurons fired.

Electrophysiology

Sharp electrodes were pulled from borosilicate glass (Sutter cat# BF150-86-10) with a Sutter p-97 pipet puller in order to obtain a resistance of 50-100 M Ω . They were then filled with 3M KCl and 40 μ M Alexa488. Animals were impaled under visualization with calcium imaging using a similar setup as in the previous experiments, except that the microscope was an upright Olympus BX51WI. Electrical signal was acquired with a MultiClamp 700B (Axon Instruments) and the software PackIO (packio.org).

Statistical methods

Statistics are indicated as average \pm SEM in figures and in the text. Cross-correlation was computed between spike trains using the MATLAB function `xcorr`. To compare the number of spikes before vs after radial contraction, we ran a two-tailed paired T-test assuming equal variance using Microsoft Excel. To compare morphological parameters, 2-tailed, paired or unpaired student T-tests were used as specified in text.

REFERENCES

1. Technau, U., and Steele, R.E. (2011). Evolutionary crossroads in developmental biology: cnidaria. *Development* 138, 2639–2648.
2. Passano, L.M., and McCullough, C.B. (1962). the Light Response and the Rhythmic Potentials of *Hydra*. *Proc. Natl. Acad. Sci. U. S. A.* 48, 1376–82.
3. Passano, L.M., and McCullough, C.B. (1963). Pacemaker Hierarchies controlling the behaviour of *Hydras*. *Nature* 199, 1174–1175.
4. Westfall, J. a, Yamataka, S., and Enos, P.D. (1971). Ultrastructural evidence of polarized synapses in the nerve net of *Hydra*. *J. Cell Biol.* 51, 318–23.
5. Westfall, J. a, Kinnamon, and Sims (1980). Neuro-neuronal gap junctions in *Hydra*. *J. Neurocytol.* 9, 725–732.
6. Westfall, J. a, and Kinnamon, J.C. (1984). Perioral synaptic connections and their possible role in the feeding behavior of *Hydra*. *Tissue Cell* 16, 355–365.
7. Westfall, J. a, Argast, D.R., and Kinnamon, J.C. (1983). Numbers, distribution, and types of neurons in the pedal disk of *Hydra* based on a serial reconstruction from transmission electron micrographs. *J. Morphol.* 178, 95–103.
8. Westfall, J.A., Wilson, J.D., Rogers, R.A., and Kinnamon, J.C. (1991). Multifunctional features of a gastrodermal sensory cell in *Hydra*: three-dimensional study. *J. Neurocytol.* 20, 251–261.
9. van Leeuwenhoek, A. (1702). Green weeds growing in water, and some animalcula found about them. *Philos. Trans. R. Soc. art IV*, 1304–1311.
10. Trembley, A. (1744). Mémoires pour servir à l’histoire d’un genre de polypes d’eau douce, à bras en forme de cornes (Leiden, Netherlands: Jean and Herman Verbeek).
11. Lenhoff, H.M. (1991). Ethel Browne , Hans Spemann , and the Discovery of the Organizer Phenomenon. *Biol. Bull.*, 72–80.
12. David, C.N. (1973). A quantitative method for maceration of *Hydra* tissue. *Wilhelm Roux Arch. für Entwicklungsmechanik der Org.* 171, 259–268.
13. Parker, G.H. (1919). *The Elementary Nervous system* (Philadelphia: J. B. Lippincott Co.).
14. Epp, L., and Tardent, P. (1978). The Distribution of Nerve Cells in *Hydra attenuata* Pall . *193*, 185–193.
15. Rushforth, N.B., and Burke, D.S. (1971). Behavioral and electrophysiological studies of *Hydra*. II. Pacemaker activity of isolated tentacles. *140*, 502–519.
16. Kass-Simon, G. (1972). Longitudinal Conduction of Contraction Burst Pulses from Hypostomal Excitation Loci in *Hydra attenuata*. *J. Comp. Physiol.* 49, 29–49.
17. Passano, L.M., and McCullough, C.B. (1965). Co-ordinating systems and behaviour in *Hydra*. II. The rhythmic potential system.
18. Kass-Simon, G., and Passano, L.M. (1978). A Neuropharmacological Analysis of the Pacemakers and Conducting Tissues of *Hydra attenuata*. *79*, 71–79.
19. Kay, J.C., and Kass-Simon, G. (2009). Glutamatergic transmission in *Hydra*: NMDA/D-serine affects the electrical activity of the body and tentacles of *Hydra vulgaris* (Cnidaria, Hydrozoa). *Biol. Bull.* 216, 113–25.
20. Shibley, G. (1969). Gastrodermal contractions correlated with rhythmic potentials and prelocomotor bursts in *Hydra*. *Am Zool.* 9, 586.
21. Haug, G. (1933). Die Lichtreaktionen der Hydren (*ChloroHydra viridissima* und

- Pelmato*Hydra* oligactis). *Z. vergleich Physiol* 19, 246–303.
22. Ewer, R.F. (1947). On the functions and mode of action of the nematocysts of *Hydra*. *Proc. zool. Soc. Lond.* 117, 365–376.
 23. Lasker, H.R., Syron, J.A., and Clayton, W.S. (1982). The feeding response of *Hydra viridis*: effects of prey-density on capture rates. *Biol. Bull.* 162, 290–298.
 24. Bullock, T.H., and Horridge, G.A. (1965). *Structure and Function in the Nervous System of Invertebrates* (San Francisco and London: W.H. Freeman a. Comp. Ltd).
 25. Kass-Simon, G., and Diesl, V.K. (1977). Spontaneous and evoked potentials from dissociated epithelial cells of *Hydra*. *Nature* 265, 75–77.
 26. Campbell, R.D., Josephson, R.K., Schwab, W.E., and Rushforth, N.B. (1976). Excitability of nerve-free *Hydra*. *Nature* 262, 388–390.
 27. Ruggieri, R.D., Pierobon, P., and Kass-Simon, G. (2004). Pacemaker activity in *Hydra* is modulated by glycine receptor ligands. *Comp. Biochem. Physiol. A. Mol. Integr. Physiol.* 138, 193–202.
 28. Chapman, J.A., Kirkness, E.F., Simakov, O., Hampson, S.E., Mitros, T., Weinmaier, T., Rattei, T., Balasubramanian, P.G., Borman, J., Busam, D., *et al.* (2010). The dynamic genome of *Hydra*. *Nature* 464, 592–6.
 29. Sakarya, O., Armstrong, K.A., Adamska, M., Adamski, M., Wang, I.F., Tidor, B., Degnan, B.M., Oakley, T.H., and Kosik, K.S. (2007). A Post-Synaptic Scaffold at the Origin of the Animal Kingdom. *PLoS One* 2, e506.
 30. Wittlieb, J., Khalturin, K., Lohmann, J.U., Anton-Erxleben, F., and Bosch, T.C.G. (2006). Transgenic *Hydra* allow in vivo tracking of individual stem cells during morphogenesis. *Proc. Natl. Acad. Sci. U. S. A.* 103, 6208–11.
 31. Yuste, R., and Katz, L.C. (1991). Control of postsynaptic Ca²⁺ influx in developing neocortex by excitatory and inhibitory neurotransmitters. *Neuron* 6, 333–344.
 32. Martínez, D.E. (1998). Mortality patterns suggest lack of senescence in *Hydra*. *Exp. Gerontol.* 33, 217–225.
 33. Layden, M.J., Rentzsch, F., and Röttinger, E. (2016). The rise of the starlet sea anemone *Nematostella vectensis* as a model system to investigate development and regeneration. *Wiley Interdiscip. Rev. Dev. Biol.* 5, 408–428.
 34. Dana, C.E., Glauber, K.M., Chan, T.A., Bridge, D.M., and Steele, R.E. (2012). Incorporation of a horizontally transferred gene into an operon during cnidarian evolution. *PLoS One* 7, e31643.
 35. Juliano, C.E. (2014). Generation of Transgenic *Hydra* by Embryo Microinjection. *J. Vis. Exp.* 91, e51888.
 36. Plachetzki, D.C., Fong, C.R., and Oakley, T.H. (2012). Cnidocyte discharge is regulated by light and opsin-mediated phototransduction. *BMC Biol.* 10, 17.
 37. Passano, L.M., and McCullough, C.B. (1964). Co-ordinating systems and behaviour in *Hydra*. I. Pacemaker system of the periodic contractions. *J. Exp. Biol.* 41, 643–664.
 38. Hufnagel, L., and Kass-Simon, G. (1976). The Ultrastructural Basis for the Electrical Coordination Between Epithelia of *Hydra*. In *Coelenterate Ecology and Behavior*, G. O. Mackie, ed. (New York: Springer US), pp. 695–704.
 39. Tardent, P., and Weber, C. (1976). A qualitative and quantitative inventory of nervous cells in *Hydra attenuata* Pall. In *Coelenterate Ecology and Behavior*, G. O. Mackie, ed. (New York: Springer US), pp. 501–502.

40. Hansen, G.N., Williamson, M., and Grimmelikhuijzen, C.J.P. (2002). A new case of neuropeptide coexpression (RGamide and LWamides) in *Hydra*, found by whole-mount, two-color double-labeling in situ hybridization. *Cell Tissue Res.* 308, 157–65.
41. Norgaard Hansen, G., Williamson, M., and Grimmelikhuijzen, C.J.P. (2000). Two-color double-labeling in situ hybridization of whole-mount *Hydra* using RNA probes for five different *Hydra* neuropeptide prohormones: evidence for colocalization. *Cell Tissue Res.* 301, 245–253.
42. Koizumi, O., Itazawa, M., Mizumoto, H., Minobe, S., Javois, L.C., Grimmelikhuijzen, C.J., and Bode, H.R. (1992). Nerve ring of the hypostome in *Hydra*. I. Its structure, development, and maintenance. *J. Comp. Neurol.* 326, 7–21.
43. Yum, S., Takahashi, T., Koizumi, O., Ariura, Y., Kobayakawa, Y., Mohri, S., and Fujisawa, T. (1998). A novel neuropeptide, Hym-176, induces contraction of the ectodermal muscle in *Hydra*. *Biochem. Biophys. Res. Commun.* 248, 584–590.
44. Guertin, S., and Kass-Simon, G. (2015). Extraocular spectral photosensitivity in the tentacles of *Hydra vulgaris*. *Comp. Biochem. Physiol. Part A Mol. Integr. Physiol.* 184, 163–170.
45. Hopfield, J.J. (1982). Neural networks and physical systems with emergent collective computational abilities. *Proc. Natl. Acad. Sci. U. S. A.* 79, 2554–2558.
46. Hopfield, J.J., and Tank, D.W. (1985). “Neural” computation of decisions in optimization problems. *Biol. Cybern.* 52, 141–152.
47. Alivisatos, A.P., Chun, M., Church, G.M., Greenspan, R.J., Roukes, M.L., and Yuste, R. (2012). The brain activity map project and the challenge of functional connectomics. *Neuron* 74, 970–4.
48. Venkatachalam, V., Ji, N., Wang, X., Clark, C., Mitchell, J.K., Klein, M., Tabone, C.J., Florman, J., Ji, H., Greenwood, J., *et al.* (2016). Pan-neuronal imaging in roaming *Caenorhabditis elegans*. *Proc. Natl. Acad. Sci. U. S. A.* 113, E1082-8.
49. Nguyen, J.P., Shipley, F.B., Linder, A.N., Plummer, G.S., Liu, M., Setru, S.U., Shaevitz, J.W., and Leifer, A.M. (2015). Whole-brain calcium imaging with cellular resolution in freely behaving *Caenorhabditis elegans*. *Proc. Natl. Acad. Sci. U. S. A.*, 33.
50. Prevedel, R., Yoon, Y.-G., Hoffmann, M., Pak, N., Wetzstein, G., Kato, S., Schrödel, T., Raskar, R., Zimmer, M., Boyden, E.S., *et al.* (2014). Simultaneous whole-animal 3D imaging of neuronal activity using light-field microscopy. *Nat. Methods* 11, 727–30.
51. Schrödel, T., Prevedel, R., Aumayr, K., Zimmer, M., and Vaziri, A. (2013). Brain-wide 3D imaging of neuronal activity in *Caenorhabditis elegans* with sculpted light. *Nat. Methods* 10, 1013–20.
52. Chhetri, R.K., Amat, F., Wan, Y., Höckendorf, B., Lemon, W.C., and Keller, P.J. (2015). Whole-animal functional and developmental imaging with isotropic spatial resolution. *Nat. Methods* 12, 1171–1178.
53. Grover, D., Katsuki, T., and Greenspan, R.J. (2016). Flyception: imaging brain activity in freely walking fruit flies. *Nat. Methods* 13, 569–572.
54. Ahrens, M.B., Li, J.M., Orger, M.B., Robson, D.N., Schier, A.F., Engert, F., and Portugues, R. (2012). Brain-wide neuronal dynamics during motor adaptation in zebrafish. *Nature* 485, 471–7.
55. Dunn, T.W., Mu, Y., Narayan, S., Randlett, O., Naumann, E.A., Yang, C.T., Schier, A.F., Freeman, J., Engert, F., and Ahrens, M.B. (2016). Brain-wide mapping of neural activity

- controlling zebrafish exploratory locomotion. *Elife* 5, 1–29.
56. Wolf, S., Supatto, W., Debrégeas, G., Mahou, P., Kruglik, S.G., Sintès, J.-M., Beaurepaire, E., and Candelier, R. (2015). Whole-brain functional imaging with two-photon light-sheet microscopy. *Nat. Methods* 12, 379–380.
 57. Panier, T., Romano, S.A., Olive, R., Pietri, T., Sumbre, G., Candelier, R., and Debrégeas, G. (2013). Fast functional imaging of multiple brain regions in intact zebrafish larvae using selective plane illumination microscopy. *Front. Neural Circuits* 7, 65.
 58. Portugues, R., Feierstein, C.E., Engert, F., and Orger, M.B. (2014). Whole-brain activity maps reveal stereotyped, distributed networks for visuomotor behavior. *Neuron* 81, 1328–1343.
 59. Tomer, R., Lovett-Barron, M., Kauvar, I., Andalman, A., Burns, V.M., Sankaran, S., Grosenick, L., Broxton, M., Yang, S., and Deisseroth, K. (2015). SPED Light Sheet Microscopy: Fast Mapping of Biological System Structure and Function. *Cell* 163, 1796–1806.
 60. Mcfarlane, I.D. (1969). Two Slow Conduction Systems in the Sea Anemone *Calliactis Parasitica*. *J. Exp. Biol.* 51, 377–385.
 61. Miller, J.-E.K., Ayzenshtat, I., Carrillo-Reid, L., and Yuste, R. (2014). Visual stimuli recruit intrinsically generated cortical ensembles. *Proc. Natl. Acad. Sci.* 111, E4053–61.
 62. Passano, L.M. (1963). Primitive Nervous Systems. *Proc. Natl. Acad. Sci. U. S. A.*, 306–313.
 63. Schindelin, J., Arganda-carreras, I., Frise, E., Kaynig, V., Longair, M., Pietzsch, T., Preibisch, S., Rueden, C., Saalfeld, S., Schmid, B., *et al.* (2012). Fiji : an open-source platform for biological-image analysis. *Nat. Methods* 9, 676–682.
 64. Dupre, C., and Yuste, R. (2017). Non-overlapping neural networks in *Hydra vulgaris*. *Curr. Biol.*, 1–13.
 65. Khalturin, K., Anton-Erxleben, F., Milde, S., Plötz, C., Wittlieb, J., Hemmrich, G., and Bosch, T.C.G. (2007). Transgenic stem cells in *Hydra* reveal an early evolutionary origin for key elements controlling self-renewal and differentiation. *Dev. Biol.* 309, 32–44.
 66. Edelstein, A., Amodaj, N., Hoover, K., Vale, R., and Stuurman, N. (2010). Computer control of microscopes using μ Manager. *Curr. Protoc. Mol. Biol.* 92, 14.20.1–14.20.17.
 67. Schneider, C.A., Rasband, W.S., and Eliceiri, K.W. (2012). NIH Image to ImageJ: 25 years of image analysis. *Nat. Methods* 9, 671–675.

APPENDIX A: SUPPLEMENTAL FIGURES

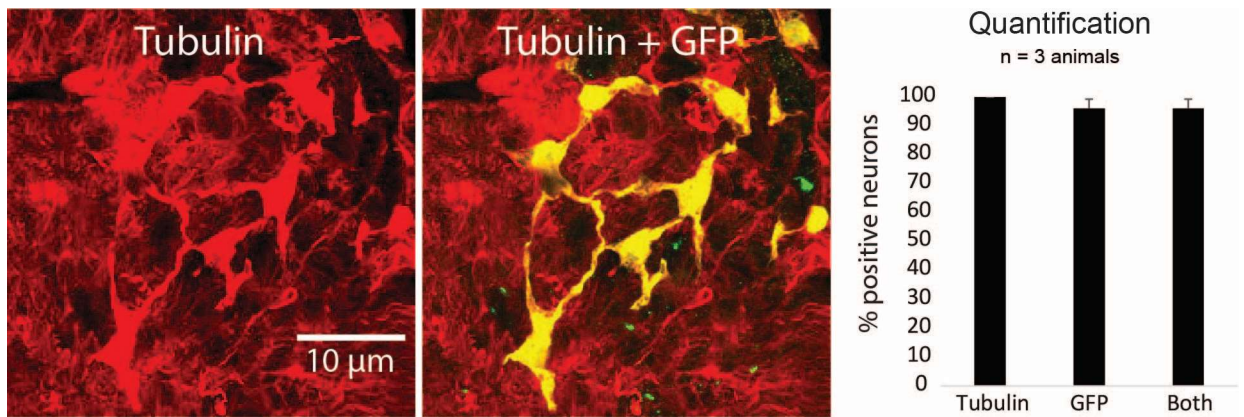


Figure S 1: Percentage of transgenic neurons. Related to Figure 4

Left: Immunostaining with acetylated alpha-tubulin antibody only. Middle: Immunostaining with both GCaMP6s and acetylated alpha-tubulin antibodies. Right: Overlap between the two stainings. Error bars indicate SEM.

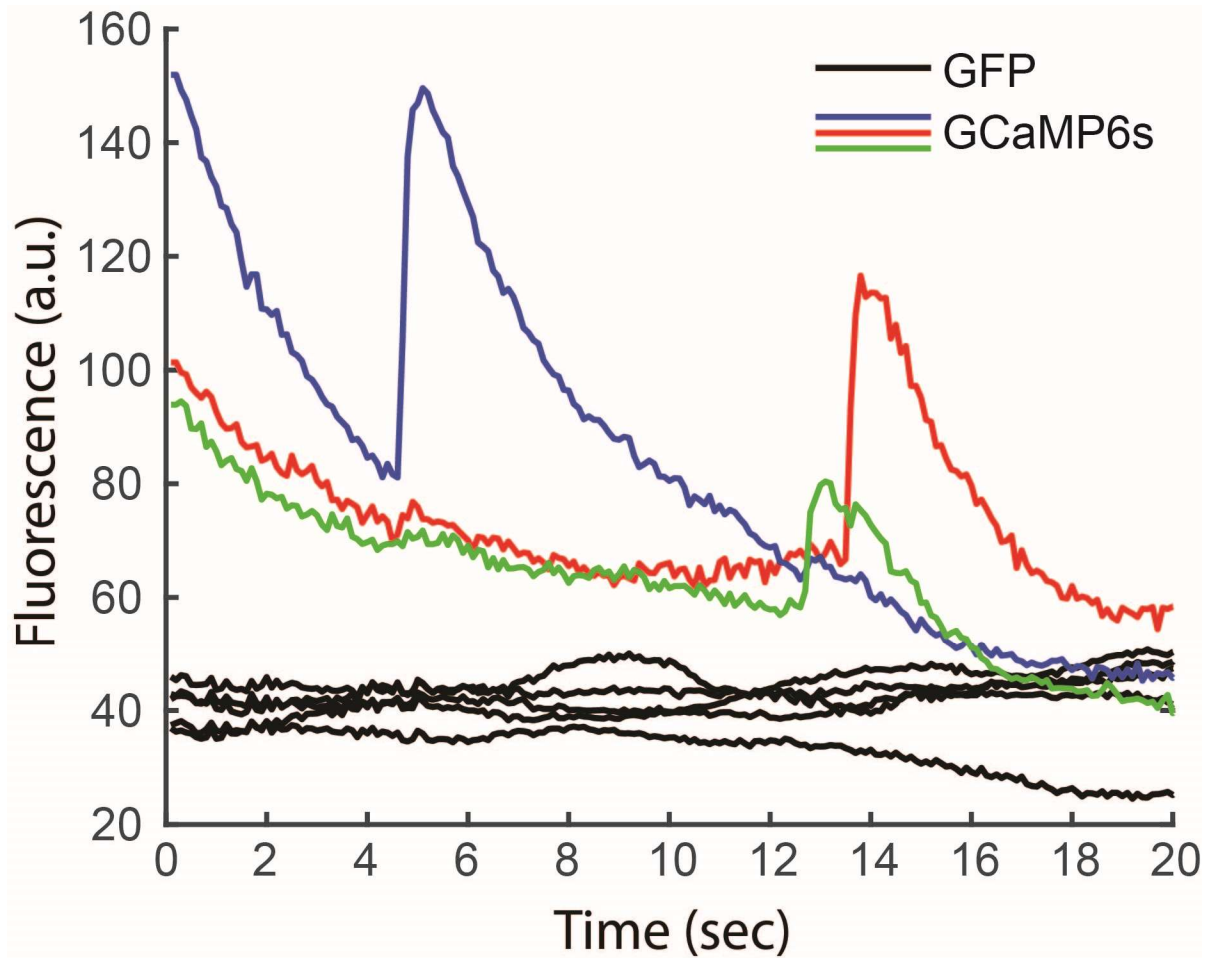


Figure S 2: Fluorescence transients in cells expressing GFP compared to GCaMP6s.

Related to Figure 4

The green, red and blue traces correspond to neurons expressing GCaMP6s which belong to the RP1, RP2 and CB groups, respectively. The black traces correspond to 5 neurons of another transgenic line expressing GFP in neurons. Both GFP and GCaMP6s signals were recorded during the same behavioral sequence: the last two pulses of a contraction burst, followed by about 15 seconds of elongation.

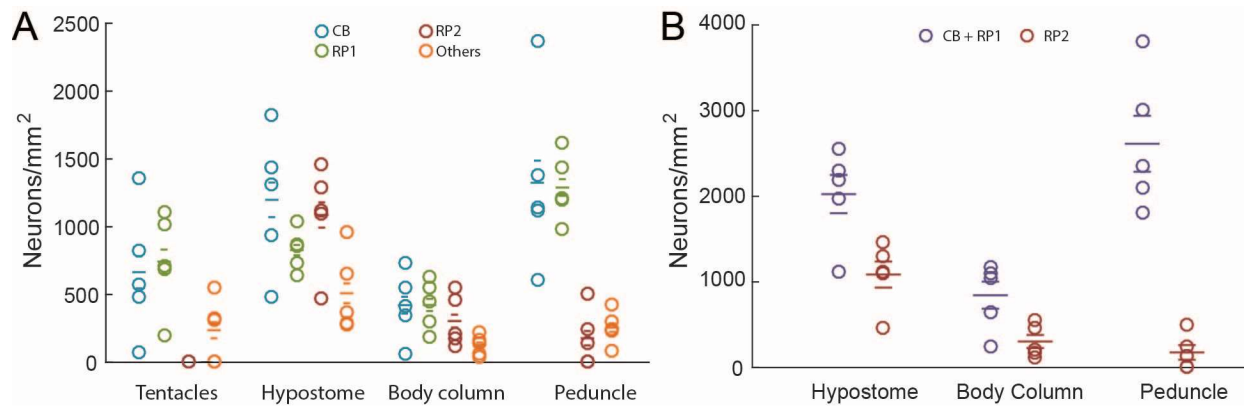


Figure S 3: Distribution of neuronal density. Related to Figure 7

Neuronal density in different animal parts, according to each cell type (A) and when RP1 and CB are combined (B). A. The density of RP1 and CB neurons is higher in the hypostome and the peduncle than in the body column. The density of RP2 neurons is not significantly different between the peduncle and the body column, but higher in the hypostome. B. RP1 + CB versus RP2 give density patterns similar to the patterns reported in Epp and Tardent (1978) for ectoderm versus endoderm. $n = 1023$ neurons compared over 5 animals. Wide bars indicate mean, narrow bars indicate SEM

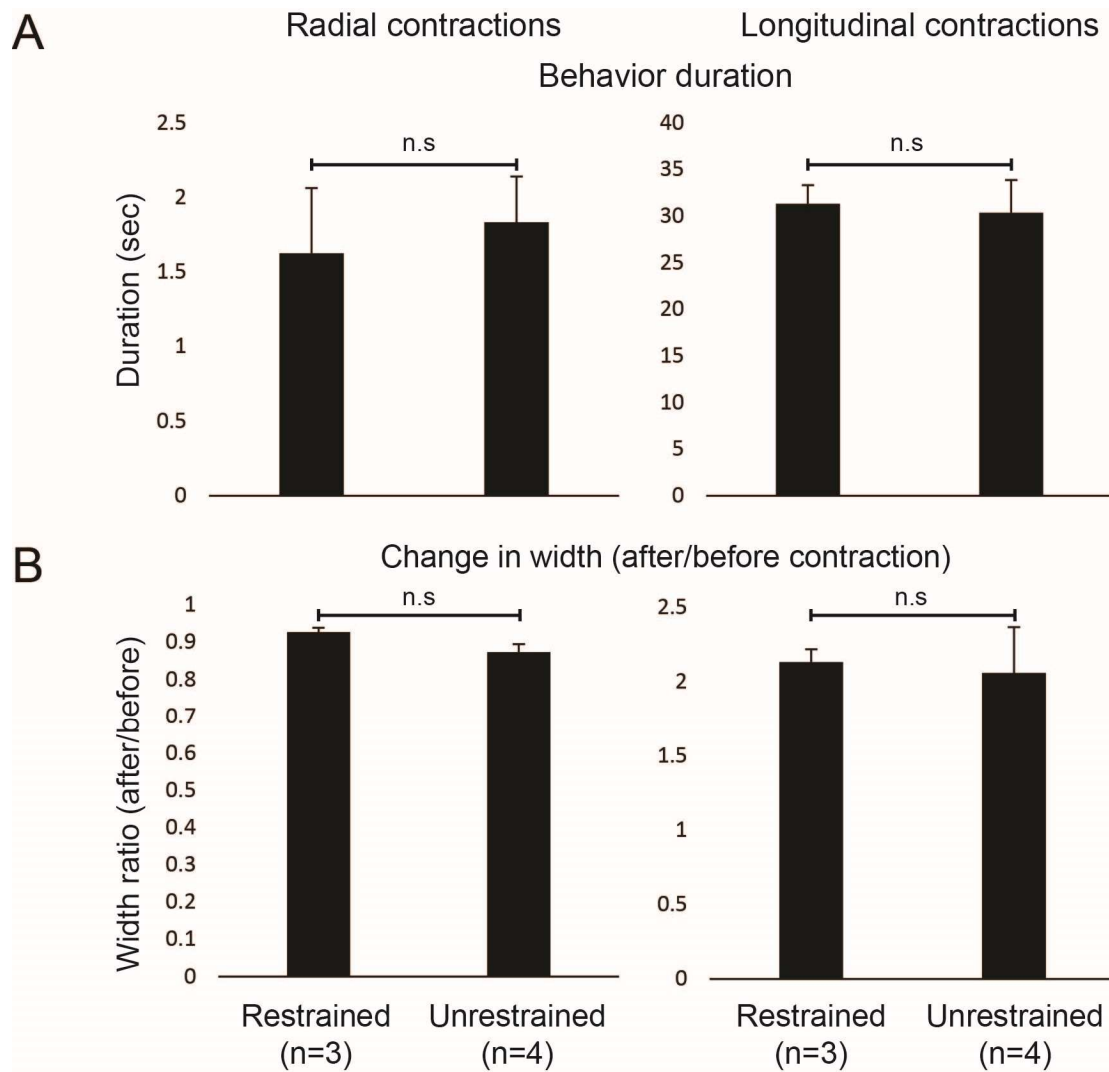


Figure S 4: Differences in behavior between restrained and unrestrained preparation.

Related to Figure 4

A) Duration of radial and longitudinal contractions in restrained vs unrestrained preparation. B)

Change in width of the animal following radial and longitudinal contractions in restrained vs

unrestrained preparation. Unpaired T-Test was used, with n.s = not significant ($P > 0.05$).

APPENDIX B: SUPPLEMENTAL MOVIES LEGENDS

Movie S1. Calcium imaging in Hydra, Related to Figure 1

The animal is placed between two coverslips separated by a 100 μ m spacer and imaged with a fluorescence dissecting microscope with an exposure time of 100ms. To generate this movie, the raw movie was averaged by 5 frames bins and then converted into mp4 format. One second in the movie corresponds to 12.5 seconds in real time. Calcium traces shown in Figure 1 were extracted from the first 200 frames of the raw movie, which correspond to the first 40 frames of this movie. Scale bar = 100 μ m.

Movie S2. Tracking neurons during behavior, Related to Figure 1

The position of the 620 neurons was tracked over 20 seconds using TrackMate. Each circle marks one neuron, and the color corresponds to the functional group. Green = RP1, Red = RP2, Blue = CB, light blue = CB2, yellow = others, including subtentacle network, white = nematocytes. 1 second in the movie corresponds to 5 seconds in real time. Scale bar = 100 μ m.

Movie S3. Elongation response to light, Related to Figure 5

A dark habituated Hydra responds to a light stimulus by elongating its body column. The frequency of the RP1 system is very low before elongation, and increases sharply at the onset of elongation and stays high during elongation. One second in the movie corresponds to 25 seconds in real time. Scale bar = 200 μ m

Movie S4. 3 examples of radial contraction, Related to Figure 5

Radial contraction behavior includes opening of the mouth of the animal, followed by a rapid contraction of the body column in the medial-lateral plane. The frequency of the RP2 system

increases until radial contraction, after which it decreases sharply. One second in the movie corresponds to 25 seconds in real time. Scale bar = 100 μm .

Movie S5. Behavior in unrestrained environment, Related to Figure 5

Radial contraction is a behavior that is more difficult to observe because it cannot be triggered easily. This movie shows that in addition to occurring when the animal is restrained between two coverslips (Figure 4), it also happens in an unrestrained animal. 1 second in the movie corresponds to 2.4 seconds in real time. Radial contraction happens at $T = 3$ sec. Scale bar = 100 μm .